ELSEVIER

Coordination Chemistry Reviews
177 (1998) 219–256

COORDINATION CHEMISTRY REVIEWS

Mechanistic roles of metal-to-ligand charge-transfer excited states in organometallic photochemistry

Antonín Vlček Jr. *

Department of Chemistry, Queen Mary and Westfield College, University of London, Mile End Road, London E1 4NS, UK

Received 21 January 1998; accepted 2 July 1998

Contents

* Tel.: +44-171-7753260; Fax: +44-181-9818745; e-mail: a.vlcek@qmw.ac.uk.

PII: S0010-8545(98)00187-8

Abstract

Metal-to-ligand charge-transfer (MLCT) excitation of organometallic and coordination complexes has diverse chemical and physical consequences, depending on the molecular structure and the medium. It can promptly start an ultrafast ligand dissociation, populate a long-lived, charge-separated, 3MLCT state that shows typical reactivity of the oxidised metal atom or reduced ligand (electron transfer, associative substitution, oxidative addition), or lead to a long-lived 3MLCT state from which another, more reactive, excited state is populated thermally. Alternatively, a MLCT state may be unreactive with respect to the breaking or formation of metal–ligand bonds but engaged in electron- or energy-transfer reactions or just decaying to the ground state. The MLCT photochemistry is discussed in terms of the bonding properties and dynamics of the MLCT excited states which are, to some extent, dependent on interactions with other excited states of different orbital origins (LF, $\sigma\pi^*$, IL). An examination of actual mechanistic roles of MLCT states in representative classes of photochemical reactions allows to outline more general relations between the molecular structure and photoreactivity of MLCT-active organometallic compounds.

Keywords: Metal-to-ligand charge-transfer; Excited state dynamics; Photochemistry; Organometallics

1. Introduction

Typical metal-to-ligand charge-transfer (MLCT) excitation involves a $d_\pi \rightarrow \pi^*$ transition whereby an electron is excited from an occupied, predominantly metal-localised, d_π orbital to a vacant, ligand-localised orbital, usually of a π^* character [1–9]. The MLCT excitation then results in a virtual oxidation of the metal atom and a concomitant reduction of the ligand:

$$A_nM - L \xrightarrow{h\nu} A_nM^+ - L^-, \quad (1)$$

where A represents a spectator ligand, not directly involved in the MLCT process. Indeed, excited state resonance Raman, IR or UV–Vis absorption spectra of complexes with long-lived MLCT excited states often show features characteristic of reduced acceptor ligands and/or oxidised A_nM fragments. In reality, the charge separation in the MLCT excited state is never complete, being somewhat diminished by the $M \rightarrow L$ π back-bonding which mixes the donor and acceptor orbitals of the metal atom and the ligand, respectively, and by compensating effects of accompanying changes in the overall electron density distribution and solvation [6,10–13]. Electroabsorption spectra and studies of the excited state distortion have indicated [11,14,15] that the charge separation in MLCT excited states usually occurs to the extent of 70–98%, although more extensive M–L delocalisation may be encountered exceptionally [6,11,16,17].

MLCT electronic transitions are common to many coordination or organometallic compounds of low-valent metal atoms with electron accepting ligands like α,α'-diimines (including 2,2′-bipyridine (bpy), 1,10-phenanthroline (phen) and related polypyridyls and polyazines), some pyridine derivatives, 4,4′-bipyridine, *N*-

alkyl-4,4′-bipyridinium cations, isonitriles, CO, *o*-quinones or semiquinones, olefins, acetylenes, and many others. MLCT transitions are usually spectroscopically strongly allowed, manifested by intense absorption bands in the visible or near UV spectral regions [2]. Irradiation into MLCT transitions is thus a very efficient and convenient way to collect light energy.

What are the chemical consequences of MLCT excitation? The simple one-electron description of a MLCT excited state as a charge separated species (Eq. (1)) does not suggest any major labilisation of metal–ligand bonds. Neither strongly bonding molecular orbitals are depopulated nor strongly antibonding ones populated. The virtual oxidation makes the metal centre more Lewis-acidic and some strengthening of the metal–ligand σ bonds on MLCT excitation may thus be expected. However, this effect could be compensated for by a concomitant weakening of $M \rightarrow A$ and/or $M \rightarrow L$ π back-bonding. The π^* ligand orbital is usually delocalised over the acceptor ligand. Hence, its population by MLCT excitation causes only a limited molecular distortion which enables a nonradiative decay of MLCT excited states [18–20] but is not sufficient to cause a chemical reactivity.

Indeed, MLCT excited states of many coordination and organometallic compounds are chemically stable. They decay back to the ground state, often with a remarkable emission. The lifetimes range from tens of nanoseconds to microseconds. Photochemical reactivity is dominated by well known energy- or electron-transfer [1,3] reactions which usually occur without any transformation of the photoactive molecules themselves. However, this electron- and energy-transfer reactivity of long-lived, inherently stable, MLCT states represents only one face of MLCT-induced photochemistry. In fact, the MLCT excitation of many organometallic and coordination compounds does cause productive photochemical reactions in which metal–ligand bonds are broken and/or formed. MLCT-induced photochemical substitution, isomerisation, radical formation, ligand annation, oxidative addition and reactions of coordinated ligands are now known [1,9,21–24]. Most of the early research on the MLCT photochemical reactivity has concentrated on ligand substitutions which take place from ligand field (LF) excited states that are populated thermally from the primarily excited MLCT state [1,22–28]. This is, for example, the case of the photosubstitution of $Ru(bpy)_3 2+$ and some of its analogues [8,29–32], as well as of $[Ru(NH_3)_5(py–X)]2+$ [22–24,28], or $W(CO)_5(py–X)$ [1,33–37] where py–X stands for pyridine 4-substituted with electron-accepting groups. Analogously, a *trans–cis* isomerisation of a 4-styrylpyridine ligand (sp) in complexes like $W(CO)_5(sp)$, $Re(Cl)(CO)_3(sp)_2$ or $[Ru(bpy)_2(sp)_2]2+$ was attributed to a population of an intraligand (IL) state following a MLCT excitation [1,24,38]. On the other hand, the photochemical reactivity of many organometallic carbonyl–diimine or isonitrile complexes was found to occur directly from the optically excited MLCT state. Thus, $M(CO)_4$(diimine) [39–47] or $M(CNPh)_6$ [48–51]; M = Cr, Mo, W; $Fe(CO)_3$(diimine) [27], $Fe(CO)_3(N_4Me_2)$ [52,53], or $Mn(E)(CO)_3$(diimine); E = Cl, Br, Me; [54–56] all undergo prompt ligand dissociation on MLCT excitation. An insight into the mechanism of a metal–ligand bond activation by MLCT excitation is now emerging from a combination of theoretical and experimental studies.

Recent theoretical work has even suggested [57,58] that the CO photodissociation from the Cr, Mo or W hexacarbonyls, long regarded as a prototypical reaction of LF states [1], occurs actually from M → CO MLCT excited states. This would point to an even broader role of MLCT excited states in organometallic photochemistry. Still different photoreactivity, metal–metal or metal–alkyl bond homolysis could be induced by MLCT excitation of $M(E)(CO)_3$(diimine) complexes; M = Re or Mn, E = Et, ^{i}Pr, benzyl, $Mn(CO)_5$ or $Re(CO)_5$ [6,7,56,59–64] or $Os_3(CO)_{10}$(diimine) clusters [65–67]. On the other hand, photochemical oxidative additions have been described for $Pt(Me)_2$(phen) [68] and related planar complexes [69,70], as well as for photocatalytically important $Rh(PMe_3)_2(CO)(Cl)$ species [71–73].

It clearly follows that MLCT excitation is able to activate organometallic molecules in several different ways, inducing rather diverse photochemical reactivity. The actual MLCT photochemistry observed depends mostly on the structure of the photoactive molecules and, to some extent, it may be tuned by other factors, namely the excitation wavelength or the nature of the medium. The very existence of various pathways of MLCT photochemistry is mechanistically rather intriguing. It contradicts the simple one-electron model of MLCT excitation that predicts MLCT excited states to be long-lived and inherently stable. Herein, the diverse chemical consequences of MLCT excitation will be explored and ways that it may activate molecules of organometallic and coordination compounds towards potentially useful photochemical reactivity will be examined. The emphasis will be on the mechanistic understanding of the MLCT photochemistry and on its new implications to our views on the properties, behaviour and dynamics of excited states of organometallic and coordination compounds (Fig. 1).

2. General aspects of MLCT excited state dynamics

According to the Franck–Condon principle, irradiation into the MLCT electronic transition excites the complex molecule without any accompanying change in nuclear geometry and solvation. However, because of the electron density redistribution and charge separation caused by the MLCT excitation, the ground state geometry is energetically unfavourable for the MLCT exited state. Hence, the Franck–Condon excited molecule finds itself on the potential energy surface of the MLCT excited state well above its energy minimum, in an unequlibrated nuclear geometry and arrangement of solvent molecules. Hence, the vertical excitation into the Franck–Condon excited state triggers an ultrafast evolution of the molecular geometry and of the distribution and orientation of surrounding solvent molecules towards the equilibrium situation. The ultrafast (femtosecond) initial excited state dynamics determines shapes of the electronic absorption spectra, resonance Raman excitation profiles, as well as the photoreactivity. This dynamics may be conveniently treated using time-dependent quantum mechanics, namely the technique of the wavepacket propagation on the excited state potential energy surface [74–76]. Obviously, the knowledge of the shape of the excited state potential energy surfaces is crucial for the understanding of the photochemical behaviour. Much theoretical

and computational work has been carried out to obtain representative energy surfaces for organometallic compounds [58,77–81]. Qualitatively, it is important to note that the actual shapes of MLCT potential energy surfaces along photochemical reaction coordinates could be strongly influenced by interactions with higher

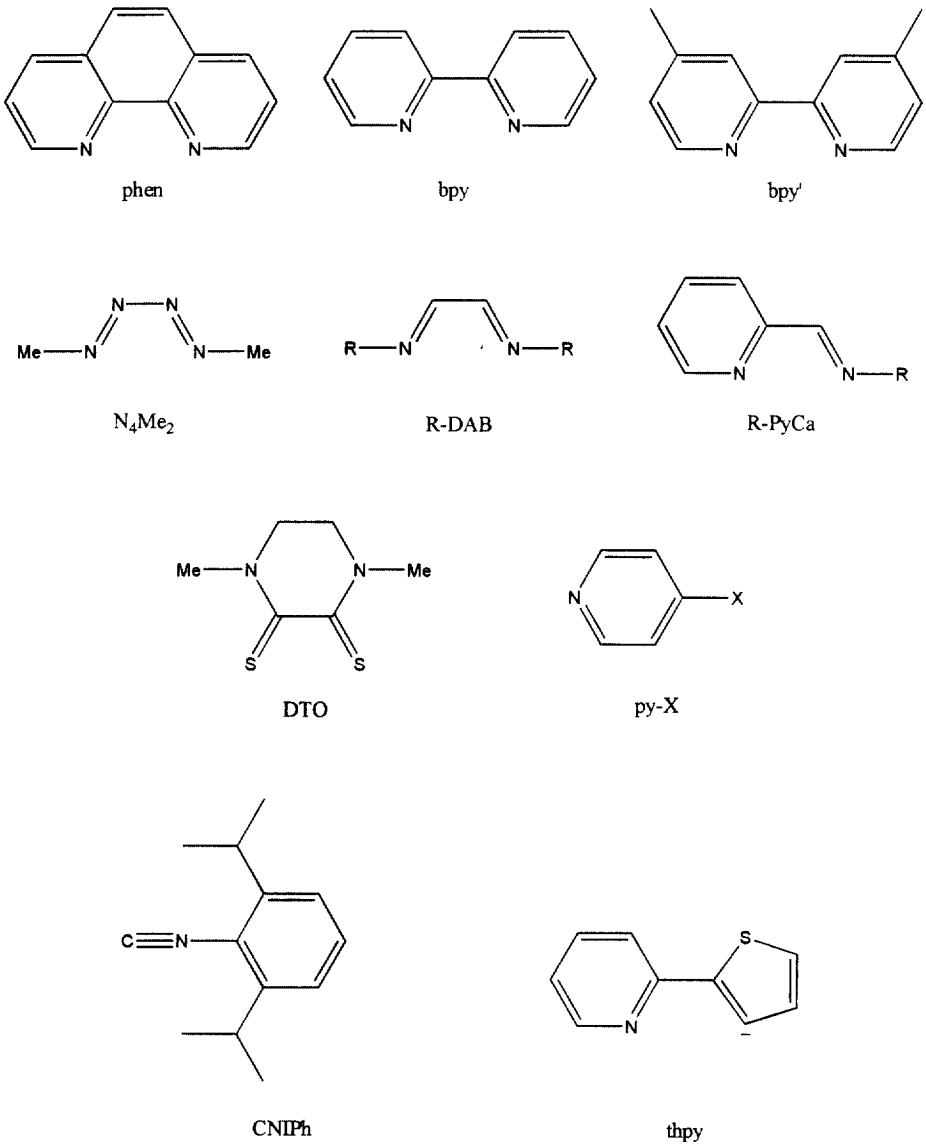

Fig. 1. Acceptor ligands and their abbreviations used in the text. Note that the term 'diimine' is used quite broadly, encompassing polypyridyl (bpy, phen, etc.), polyazine, as well as R–DAB and R–PyCa ligands.

excited states of other orbital origin. This is especially important for transition metal organometallic compounds, considering their large density of electronically excited states, low symmetry and considerable spin–orbit coupling.

In most general terms, the Franck–Condon MLCT excitation may initiate following dynamic processes:

1. Evolution on a dissociative or quasibound potential energy surface toward photochemical products, usually involving metal–ligand bond dissociation or homolysis.
2. Vibrational and electronic relaxation into a thermally-equilibrated, usually spin–triplet, MLCT excited state whose potential energy surface is bound, with a well developed energetic minimum. Such a relaxed, long-lived, MLCT excited state may have two possible fates:
   2.1. Chemical reaction.
   2.2. Radiationless and radiative decay to the ground state.

The probabilities and rates of these competitive pathways determine the overall photochemical behaviour. They depend on the structure of the excited molecule, as well on the nature of the medium (solvent) and other reaction conditions like the excitation energy (wavelength), temperature or pressure.

3. Prompt photochemical reactions from Franck–Condon MLCT excited states

3.1. Dissociation of a metal–ligand bond

Many organometallic compounds with electron-accepting ligands, namely metal carbonyls containing α-diimine ligands or metal isonitriles, undergo photochemical ligand substitution on irradiation into their low-lying MLCT absorption band. Dissociative mechanism was well established for MLCT photosubstitutions of several organometallic complexes of low-valent first-row transition metals, namely Cr^0, Mn^I, Fe^0 or Ni^0. The most common experimental arguments which indicate that the ligand dissociation is the primary photochemical step are the independence of the photochemical quantum yield on the chemical nature, size, and concentration of the entering ligand, decrease of the quantum yield with increasing external pressure (i.e. positive photochemical activation volume) and a direct detection of ligand-loss intermediates by time-resolved spectroscopic studies or during a low-temperature photolysis. Surprisingly, MLCT excitation of carbonyl–diimine complexes in most cases causes a dissociation of a spectator CO ligand which is not directly involved in the MLCT transition. Dissociation of the M–N bond was observed only for $Fe(CO)_3$('Bu–DAB) [6,27] or $Ni(CO)_2$('Bu–DAB) [6,82]. It seems to be aided by the labilising effect of the bulky 'Bu group.

A direct photochemical role of a Franck–Condon MLCT excited state in these reactions was revealed by detailed studies of combined dependencies of the quantum yield on the excitation energy, temperature, and pressure, and by time-resolved spectroscopic measurements carried out in a very broad time range, from femtoseconds to microseconds. A typical example, studied in some detail, is provided by

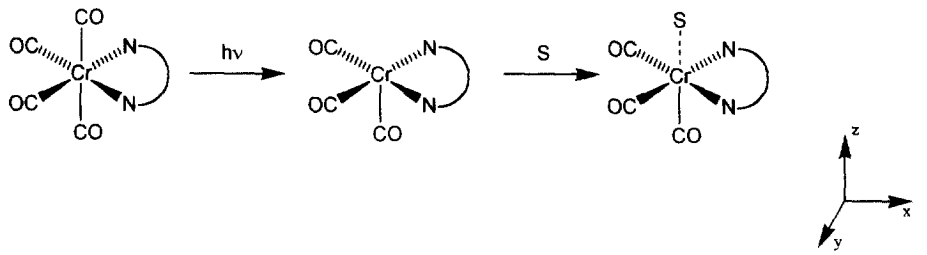

Fig. 2. Dissociative photochemical substitution of $Cr(CO)_4(bpy)$. The coordination of the solvent molecule S probably starts at later stages of the CO dissociation. In the presence of a Lewis base L, the $Cr(S)(CO)_3(bpy)$ photoproduct undergoes another, thermal, substitution to form $Cr(L)(CO)_3(bpy)$ as a stable product. Typically, L = phosphine or phosphite. The axes orientation shown is used throughout this paper.

$Cr(CO)_4(bpy)$ [39–41,45,83], see Figs. 2–4. The photochemistry of $Ni(CO)_2$-(diimine) complexes [6,82] also implies an inherent MLCT reactivity since MLCT states are the only low-lying excited states available for the d10 electron configuration of the Ni0 atom.

The respective quantum yields of the CO photodissociation from $Cr(CO)_4(bpy)$ [39,40], $Fe(CO)_3(R-DAB)$; R = cyclohexyl [27], or $Fe(CO)_3(N_4Me_2)$ [52,53] and of the PhNC photodissociation from $Cr(CNPh)_6$ [48,49,51] were found to decrease as the excitation energy decreases within the narrow spectral region of the intense MLCT absorption band, see Fig. 3. This observation shows that the ligand dissociation is not preceded by any vibrational or electronic relaxation in which all the memory of the initial excitation energy would be lost. Clearly, the photochemical CO dissociation is initiated directly by the Franck–Condon MLCT excitation, being the result of a dynamic evolution on the initially populated ^{1}MLCT potential energy surface. Accordingly, the formation of the primary CO-loss photoproduct $Cr(S)(CO)_3(bpy)$ was found to be completed already within 600 fs after the MLCT excitation of $Cr(CO)_4(bpy)$ [83]. Similarly, $Cr(CNPh)_5(THF)$ is photoproduced from $Cr(CNPh)_6$ in a THF solution in less than 1 ps [50]. Stereoselectivity is another typical feature of a prompt ligand photodissociation. For $Cr(CO)_4(bpy)$, the axial CO ligand (*cis* to the Cr(bpy) plane) dissociates selectively, producing *fac*-$Cr(S)(CO)_3(bpy)$ as the only primary photoproduct [41], see Fig. 2. Notably, the weakest skeletal bonds, Cr–N, are not affected by a MLCT excitation.

The quantum yield, ϕ, of the MLCT-induced photochemical CO dissociation is often temperature-dependent, following an Arrhenius-type dependence: $\phi = \phi_0 \exp(-E_a/RT)$. Thus, the CO dissociation from a MLCT-excited $Cr(CO)_4(bpy)$ occurs with an apparent activation energy, E_a, that increases from 1350 to 1430 cm^{-1} on decreasing the excitation energy from 20 120 to 17 950 cm^{-1} [39], see Fig. 4. Smaller E_a values of 525 or 770 cm^{-1} were found for the CO dissociation induced by MLCT excitation of $Fe(CO)_3(R-DAB)$; R = cyclohexyl [27] or $Fe(CO)_3(N_4Me_2)$ [52], respectively. It follows that the potential energy surfaces of reactive MLCT excited states are not smoothly dissociative but, instead, they

contain local minima and small barriers. In this respect, the reactivity of MLCT states is rather different from that of LF states. The CO dissociation from the latter takes place with much lower or even without any energy barriers and, at the same time, with much lower preexponential factors ϕ_0 than that from MLCT states [27,39], see Fig. 4.

To sum up, CO dissociation from several carbonyl–diimine complexes of first row transition metals and a PhNC dissociation from $Cr(CNPh)_6$ occur promptly from the optically excited Franck–Condon MLCT state, in competition with its vibrational and electronic relaxation. Such a CO dissociation is a very fast, femtosecond process. It can involve a small energy barrier. The quantum yield (i.e. the probability of the CO dissociation relative to the relaxation of the Franck–Condon state) decreases with decreasing excitation energy.

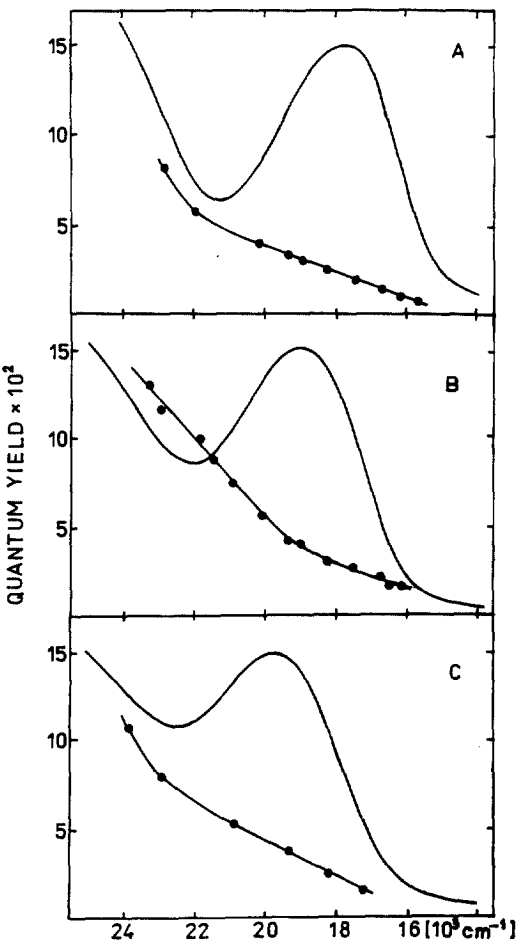

Fig. 3. Photochemical substitution of $Cr(CO)_4(bpy)$ by PPh_3: Excitation energy dependence of the quantum yield and the absorption spectrum of $Cr(CO)_4(bpy)$ measured in various solvents [39]. (A) 6:1 (v:v) C_2Cl_4:C_6H_6 mixture; (B) C_6H_6; (C) CH_2Cl_2

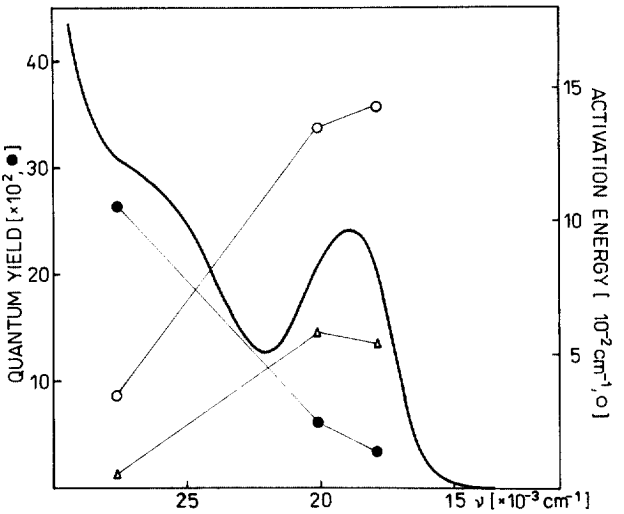

Fig. 4. Photochemical substitution of $Cr(CO)_4(bpy)$ by PPh_3 in toluene: dependence of the quantum yield ϕ, ●, (at 294 K), photochemical activation energy E_a, ○, and preexponential factor ϕ_0, △, on the excitation energy, shown together with the absorption spectrum of $Cr(CO)_4(bpy)$. The parameters E_a and ϕ_0 were obtained from the $\phi-T$ dependencies [39]. Note the different behaviour observed under the irradiation into the MLCT band (both E_a and ϕ_0 high) and at 362 nm into, presumably, LF transition (both E_a and ϕ_0 low). This points to a different nature of the reactive excited states reached by the excitation into the lowest MLCT band and into the region of the high-energy UV absorption, respectively.

Before discussing the actual mechanism of the prompt CO photodissociation, it is interesting to note the chemical effects of the one-electron reduction and oxidation, respectively, which could bear some resemblance to those of MLCT excitation [84]. Both the reduction (population of π^*) and the oxidation (depopulation of d_π) of $M(CO)_4(bpy)$; M = Cr; Mo; W; and of other diimine–carbonyl complexes to their anion- or cation-radicals, respectively, facilitate the loss of a CO ligand [85,86], but incomparably less[1] than the MLCT excitation does. In this respect, it is worth mentioning to note that the quantum yield of the MLCT-induced CO substitution falls 54 times on going from the $Cr(CO)_4(phen)$ to $Cr(CO)_4(phen-NO_2)$; $phen-NO_2$ = 5-nitro-1,10-phenanthroline [26], despite the fact the Cr atom is oxidised approximately to the same extent in the MLCT states of both complexes. However, the excited electron is largely localised on the N donor atoms of the former complex while it largely resides on the distant NO_2 group of the latter. It is evident that neither the depopulation of the weakly bonding d_π orbital nor the population of the diimine π^* orbital could alone

[1] For example, the thermal substitution of CO in $Cr(CO)_4(bpy)$ requires ca. 1.5 h reflux at 110° or a few minutes at room temperature after the reduction [85]. Oxidised $Mo(CO)_4(bpy)^+$ undergoes a CO substitution by an acetonitrile solvent molecule with a lifetime of 8.3×10^{-5} s [86].MCLT induced CO dissociation takes place in 4×10^{-13} s [83].

satisfactorily account for the huge labilising effect the MLCT excitation. The very existence of such a prompt ligand dissociation on MLCT excitation clearly defies the simple one-electron model [1] of the photochemistry of MLCT states.

To account for the prompt reactivity from the Franck–Condon excited MLCT states, it is necessary to consider the MLCT potential energy surfaces. Their possible shapes are determined by the changes in equilibrium bond lengths on MLCT excitation, as well as by interactions between the MLCT state in question and other, higher lying, excited states. Of these, the $d_\pi \rightarrow d_{\sigma^*}$ ^{1}LF state is especially important. It is very reactive, most probably unbound, with respect to the axial CO dissociation due to the population of a strongly σ-antibonding d orbital. The energy of this ^{1}LF state falls rapidly as the axial M–CO distance increases because of a strong stabilisation of the d_{σ^*} orbital which points towards the departing axial CO ligand.

Two typical situations that would give rise to a prompt MLCT photochemistry are shown schematically in Fig. 5. Compared with the ground state, the minimum of the MLCT potential energy curve along the M–CO coordinate is shifted to a longer M–CO distance. This is caused by a weakening of the M → CO π back-donation and, even more importantly, by a vibronic interaction of the MLCT state with a higher LF state through a M–CO stretching vibration. The vibronic coupling between the $d_\pi \rightarrow \pi^*$ ^{1}MLCT and $d_\pi \rightarrow d_{\sigma^*}$ ^{1}LF states leads to a mixing of the singly occupied π^* and empty d_{σ^*} orbitals. This means a partial π electron donation from the π^* orbital of the $bpy^{\bullet -}$ ligand to the empty, M–CO σ-antibonding, d_{σ^*} orbital and, hence, a strong labilisation of the M–CO bond. Such a vibronic interaction would initially lower the energy of the MLCT-excited molecule in the direction of an elongation of a single axial M–CO bond, becoming thus the primary driving force for the CO dissociation from the Franck-Condon ^{1}MLCT state. As the energy of the higher-lying LF state decreases rapidly with increasing M–CO distance, the LF and MLCT potential energy curves approach each other. The still strengthening interaction between the LF and MLCT states leads either to an avoided crossing between their potential energy surfaces (Fig. 5a) or to their mutual repulsion (Fig. 5b). The lower, originally ^{1}MLCT, surface then respectively either develops an energy barrier (Fig. 5a) or it becomes rather flat, only very weakly bound along the M–CO coordinate (Fig. 5b). In any case, an admixture of the ^{1}LF character into the ^{1}MLCT excited state gradually increases along the reaction coordinate. Propagation on such potential energy surfaces leads to a prompt formation of dissociated products, provided that the Franck–Condon state lies either above the barrier maximum or only slightly below and sufficient thermal activation energy is supplied. The system still stays on the same potential energy surface which, however, changes its character from purely ^{1}MLCT at the geometry of the Franck–Condon excitation to ^{1}LF or mixed ^{1}MLCT/^{1}LF one in the region beyond the barrier (Fig. 5a). The probability to overcome the barrier is higher if the reaction starts from higher vibronic levels and/or at higher temperatures. This model is thus in accordance with the experimentally observed increase of the quantum yield with increasing excitation energy and temperature. It also follows that the efficiency of the prompt MLCT reaction would decrease as the energy well

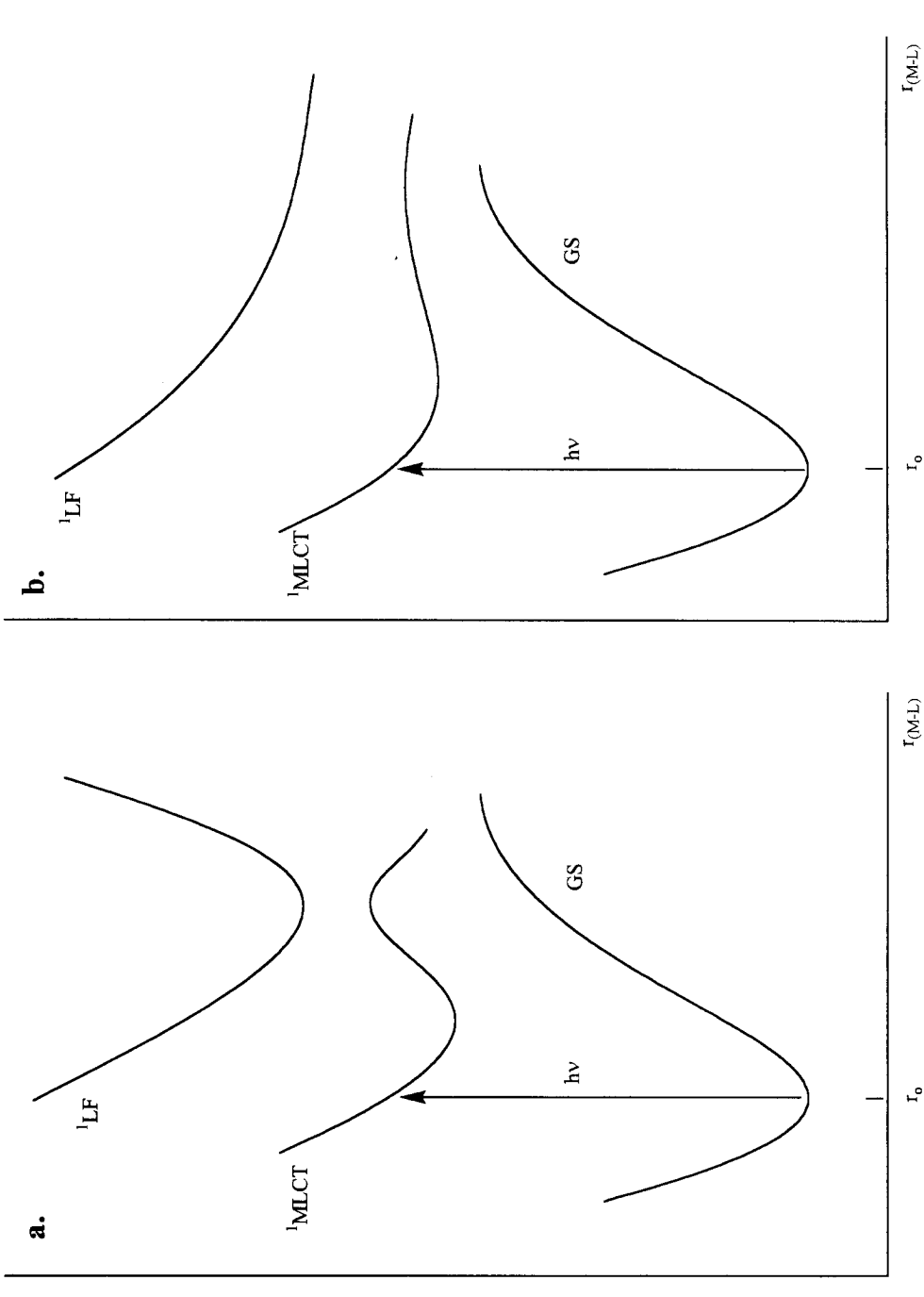

Fig. 5. Potential energy curves of a ^{1}MLCT excited state that undergoes a prompt ligand dissociation. (a) An avoided crossing between ^{1}MLCT and ^{1}LF states gives rise to a small energy barrier. (b) A repulsion between ^{1}MLCT and ^{1}LF states makes the lower, originally ^{1}MLCT, potential energy curve only weakly bound or dissociative. See text for further explanation.

on the MLCT surface deepens. This happens for complexes with low-lying and/or delocalised MLCT states. Accordingly, the quantum yield of the CO substitution in the series of $Cr(CO)_4$(diimine) complexes decreases as a function of the diimine ligand in the same order as the energy of the lowest MLCT absorption band: phen > bpy > ^{i}Pr–PyCa > ^{i}Pr–DAB > Ph–PyCa > *p*tolyl–DAB [87]. The extent of the π delocalisation over the Cr(diimine) moiety, indicated by resonance Raman spectra, increases in parallel [87].

The importance of the vibronic coupling becomes especially apparent for the more symmetrical complexes like $Cr(CO)_4$(bpy) [40]. Here, the $d_{xz} \rightarrow \pi^*$ ^{1}MLCT and $d_{xz} \rightarrow d_{z^2}$ ^{1}LF states have different symmetries in the C_{2v} geometry of the $Cr(CO)_4$(bpy) molecule, A_1 and B_2, respectively. However, they still can interact vibronically through the B_2 asymmetric stretching vibration of the axial Cr–CO bonds. This vibration lengthens asymmetrically one of the axial Cr–CO bonds that may later dissociate. Activation of the B_2 asymmetric axial Cr–CO stretching vibration by the MLCT Franck–Condon excitation thus starts the propagation of the excited molecule toward the CO-loss product and selects the one of the two, initially equivalent, axial CO ligands to dissociate.

Generally, this model predicts that the CO–loss organometallic product is formed either in a $(d_\pi)^1(d_{\sigma^*})^1$ ^{1}LF or a mixed ^{1}(LF/MLCT) excited state, corresponding to the situations shown in Fig. 5a and b, respectively. The d_{σ^*} orbital points toward the vacant site of the photoproduct, should the reaction be carried out in a high vacuum. Under usual experimental conditions, however, the solvent coordination occurs at later stages of the reaction and the product is expected to be formed in its spin-singlet $(d_\pi)^2(d_{\sigma^*})^0$ ground state. There is no need to assume any involvement of spin-triplet states in the prompt MLCT photodissociation reactions, unless the solvated ligand-loss organometallic photoproduct is formed in a spin-triplet state. In fact, a metal–ligand bond dissociation on a spin-triplet potential energy surface would be spin-forbidden for most of the reactions studied so far.

MLCT potential energy curves along the M–CO coordinate were calculated for $Mn(H)(CO)_3$(H–DAB) [78,88] with the aim of modelling the photoreactivity [56] of $Mn(R)(CO)_3$(diimine) complexes; R = alkyl. Indeed, energies of several MLCT states were found to decrease sharply from the point of the Franck–Condon excitation as the axial Mn–CO bond lengthens. At longer distances, their potential energy curves become either flat or only very weakly bound. Another detailed study of MLCT potential energy curves was performed for $Mn(Cl)(CO)_3$(H–DAB) [81]. Energy profiles along the axial Mn–CO coordinate were calculated by the DFT technique and the orbital parentage of the excited states was examined. The interaction between the $d_\pi \rightarrow \pi^*$ MLCT and $d_\pi \rightarrow d_{\sigma^*}$ LF states was indeed found to occur. It makes the dissociation energy of the axial Mn–CO bond in the MLCT state much smaller than in the ground state. However, the energy barriers for a CO dissociation from several low-lying MLCT states were calculated high and broad. Even more importantly, the ground-state of the product of the axial CO dissociation was calculated to lie energetically above the MLCT states of the parent $Mn(Cl)(CO)_3$(H–DAB) complex, at least for the isolated molecule. All these

features predict that that the photochemical dissociation of the axial CO ligand from $Mn(Cl)(CO)_3(H-DAB)$ would occur with only a small efficiency, if at all.

On the other hand, the calculations have predicted that the dissociation of the equatorial (i.e. *trans* to diimine) CO would be accompanied by a movement of the Cl ligand to the equatorial position, see Fig. 6. This theoretical result is in an excellent agreement with the experimental observation [54–56] that the CO dissociation from the complexes *fac*-Mn(E)(CO)$_3$(diimine); E = Cl, Br, or Me; occurs with an isomerisation, producing *cis*(CO,CO), *cis*(E,S)-Mn(E)(S)(CO)$_2$(diimine) as the primary photoproduct, Fig. 6. This molecular rearrangement has a large stabilising effect on the primary photoproduct. Nevertheless, the potential energy curves calculated along the equatorial Mn–CO coordinate for several low-lying MLCT states still exhibit rather large barriers. Instead of surpassing them, it was proposed [81] that a nonradiative transition occurs from the initially excited MLCT excited state to the continuum of states of the dissociated products, see Fig. 7. This continuum exists along the equatorial Mn–CO dissociation coordinate above and behind the maximum of the energy barrier of the ground state potential energy curve. For some energy values, the continuum states have resonance-enhanced amplitudes in the region of the potential energy well formed by the mininima on the ground MLCT potential energy curves [76,89]. An overlap between the vibrational levels of the MLCT excited state with these resonance-enhanced states of the dissociative continuum enables the Mn–CO bond dissociation. Coupling between the Franck–Condon MLCT state and continuum states was proposed also, although without any detailed explanation or evidence, to account for the CO photodissociation from $Fe(CO)_3(N_4Me_2)$ [52,53]. This mechanism is made possible by the topology of the potential energy surfaces in which the bound region of the MLCT potential energy surface lies above the asymptotic energy of the dissociated state. Experimental implications of a coupling between MLCT and dissociation continuum states and its importance in organometallic photochemistry still remains to be assessed and tested experimentally.

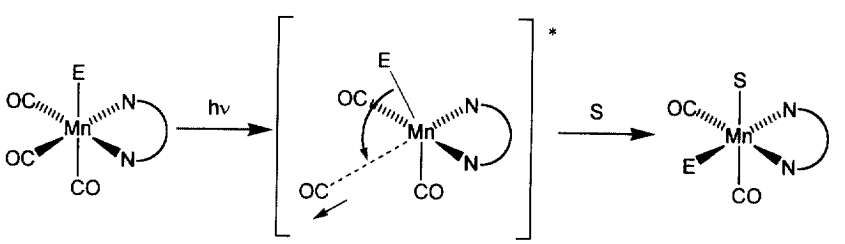

Fig. 6. Dissociative photochemical substitution/isomerisation of Mn(E)(CO)$_3$(diimine) complexes. Dissociation of the equatorial CO ligand is accompanied by a concerted movement of the axial ligand E into the equatorial plane. E = Cl, Br, I; diimine = bpy, ^{i}Pr–PyCa or ^{i}Pr–DAB. The solvent molecule S probably starts to coordinate to the axial position at later stages of the reaction. The primary photoproduct undergoes a back-reaction with CO, substitution of S by a stronger Lewis base, or a further photolysis to yield radicals [54–56]. A similar mechanism applies to the photochemistry of Ru(I)(Me)(CO)$_2$(bpy′) [91]

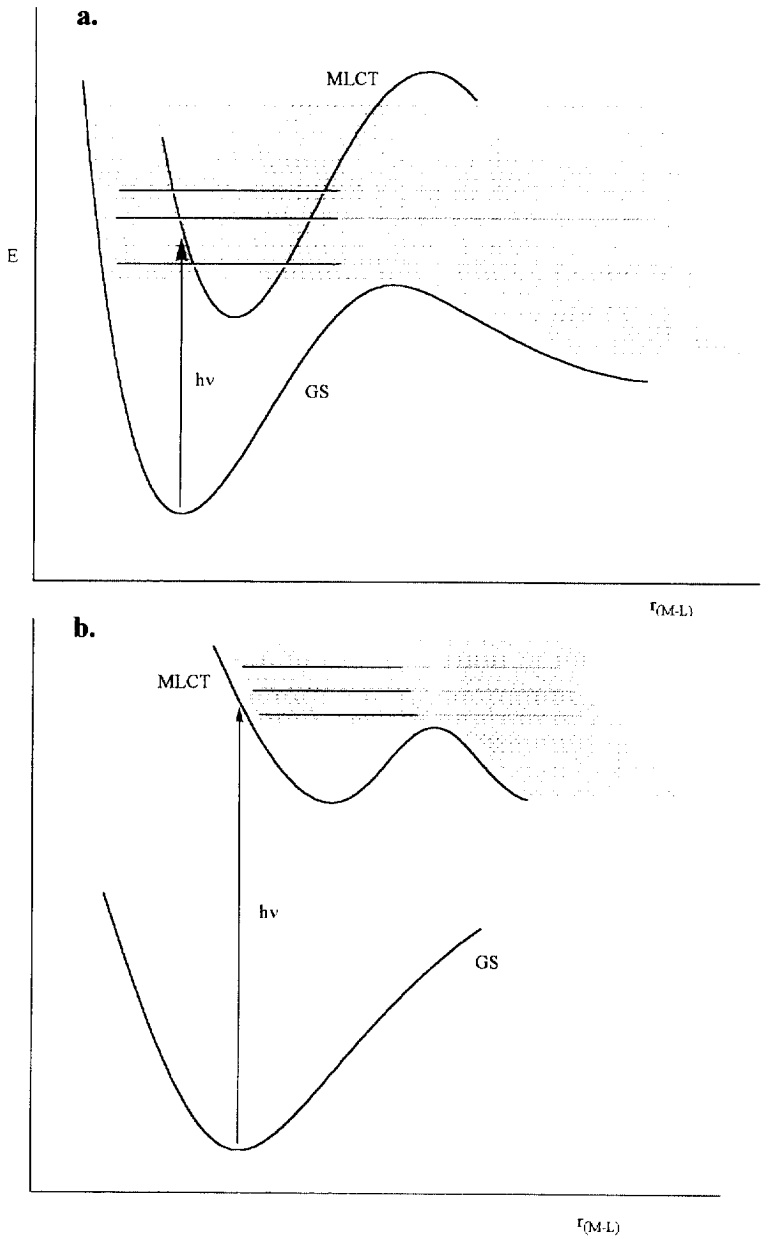

Fig. 7. Prompt ligand dissociation by a resonance coupling with states of the dissociation continuum. Grey lines correspond to continuum states whose wave functions have only a very small amplitude in the region above the energy wells formed by the potential energy curves of the ground (a) or MLCT (b) states. The wave function amplitude of some of these states is, however, strongly enhanced in this region by the resonance phenomenon [76,89]. Population of these states may cause a reaction [76,81]. (a) Coupling with states of the ground state dissociation continuum. (b) Coupling with states of the excited state dissociation continuum.

The prompt ligand dissociation from Franck–Condon ^{1}MLCT excited states seems to be well established for the complexes discussed above, i.e. $Cr(CO)_4$(diimine), $Fe(CO)_3$(R–DAB), $Fe(CO)_3(N_4Me_2)$, $Mn(E)(CO)_3$(diimine); E = Cl, Br, Me; or $Cr(CNPh)_6$. It is quite likely, however, that the metal–ligand bond dissociation from ^{1}MLCT states is much more common in organometallic photochemistry. Generally, the propensity to undergo a prompt ligand dissociation from a MLCT excited state decreases on going down the transition metal groups. Thus, the $Mn(E)(CO)_3$(diimine); E = Cl, Br, Me; complexes react readily whereas their Re analogues are, in this respect, inert [90]. Although all complexes of the type $M(CO)_4$(diimine); M = Cr, Mo, W; undergo photochemical substitution of the axial CO ligand, the quantum yield of the CO dissociation strongly decreases in the order Cr > Mo ≫ W, while the mechanism changes from dissociative to associative, vide infra. The same change of the photosubstitution mechanism from dissociative to associative with a concomitant decrease of the quantum yield occurs for $M(CNAryl)_6$ on changing M from Cr to Mo and, namely, W. The Ru^{II} carbonyl–diimine complexes are also largely inert toward CO photosubstitution with the possible exception of $Ru(Me)(I)(CO)_2$(bpy') that undergoes photochemical isomerisation after a very fast CO dissociation [91]. An efficient CO photodissociation was also found for $Ru(Cl)_2(CO)_2$(dpp); dpp = 2,5- or 2,3-bis(2-pyridyl)pyrazine and their dinuclear analogues but the mechanism was not studied [92].

All the photochemical dissociation, substitution and intramolecular oxidative addition reactions of complexes containing electron acceptors coordinated to metal atoms with d^{10} electron configuration occur directly from a MLCT excited state since other excited states are not available. For example, this is the case of the CO dissociation from $Ni(CO)_2$(diimine) [6,82], as well as of an acceptor ligand dissociation from mononuclear olefin or alkyne complexes of Pt^0 or Cu^I, including a very interesting complex $Pt^0(P(OPh)_3)_2(C_{60})$ [93]. These reactions were reviewed elsewhere [21].

An entirely different type of a MLCT excited state, called $d\sigma^*$, has recently been described for complexes containing side-on coordinated $O_2 2-$ or a bridging PhSeSePh ligand. It involves an electron excitation from a metal d-orbital to an orbital that is σ-antibonding toward an intraligand bond. Irradiation into corresponding absorption band results in a breaking of the O–O or Se–Se bond, respectively [94,95]. Although no mechanistic details are available, these reactions may be assumed to occur promptly from the initially excited $d\sigma^*$ MLCT state.

3.2. Are MLCT states responsible for the photochemistry of Group 6 metal hexacarbonyls?

The photochemical substitution of the hexacarbonyls $M(CO)_6$; M = Cr, Mo, W; have long been regarded as a textbook case of a reaction from dissociative LF excited states [1]. Photolysis of these complexes results in an efficient dissociation of one CO ligand which is completed within 150 fs after excitation [96,97]. The quantum yield does not depend on the excitation wavelength. Absorption spectra [1,98] show two very intense UV bands that belong to M → CO MLCT transitions.

A weak tail at longer wavelengths and a shoulder in the UV were attributed to LF transitions which originate in the $t_{2g} \rightarrow e_g$ excitation. The traditional picture of the photochemical mechanism assumes that the initial UV excitation into the intense M→CO MLCT transitions is followed by an ultrafast conversion to lower LF states. At some irradiation wavelengths, the LF states are reached directly. Population of the LF excited states is expected to labilise strongly the M–CO bonds by placing an electron into a σ-antibonding e_g orbital and by weakening the M→CO π back-bonding through a depopulation of the t_{2g} orbitals. The CO dissociation would thus proceed smoothly on an unbound LF potential energy surface. This mechanistic model agrees with all the experimental data available and also with the original assignment of the absorption spectra which implied that the LF states lie below the MLCT ones.

This classical mechanism has recently been challenged by the results of two theoretical studies on $Cr(CO)_6$. Both the CASSCF/CASPT2 [57] and DFT [58] calculations have predicted that the manifold of Cr→CO 1MLCT states of E_u, A_{2u}, T_{2u}, and A_{1u}, symmetries lies below the $^1T_{1u}$ MLCT state that is responsible for the first intense absorption band in the spectrum. Transitions to this group of MLCT states are symmetry forbidden and, hence, they may well account for the long-wavelength tail observed in the hexacarbonyl spectra. The lowest spin-singlet and triplet LF states were all calculated to lie above the $^1T_{1u}$ MLCT state. The DFT calculation of the potential energy curves shows that the lowest $^1T_{2u}$ MLCT state is fully dissociative with respect to the elongation of a single Cr–CO bond. This is caused by a strong mixing with a higher LF state that becomes possible as soon as the octahedral geometry of the Franck–Condon MLCT state is distorted by a lengthening of one Cr–CO bond. The potential energy curve of the LF state then falls very steeply toward that of the MLCT state as the Cr–CO distance increases. Their strong interaction makes the MLCT potential energy curve dissociative with some LF character admixed (Fig. 5b). This is manifested on an orbital level by a mixing of the π^*(CO) orbital with the $3d_{z^2}$ and $4p_z$ chromium orbitals [58]. In conclusion, the DFT calculation predicts [58] that the CO dissociation from $Cr(CO)_6$ could occur from the lowest Cr→CO MLCT excited state, despite the fact that no Cr–CO antibonding orbitals are populated. The MLCT state becomes dissociative through its interaction with a higher lying LF state, essentially in a similar way to the M→diimine MLCT states of the carbonyl–diimine complexes discussed above. However, because of the shape of the potential energy surfaces and strength of the interaction, no avoided crossing and, hence, no energy barrier occurs along the reaction coordinate [58]. This situation is shown schematically in Fig. 5b. It is also useful to view the CO photodissociation from $Cr(CO)_6$ as being initiated by a vibronic coupling between the MLCT and LF states which activates an asymmetric Cr–CO stretching vibration. This vibronic interaction causes the initial sharp fall of the MLCT state energy and it also selects the CO ligand that will dissociate.

A similar mechanism almost certainly applies to the photochemistry of the Mo and W hexacarbonyls and to the dissociation of an ArNC ligand from $Cr(CNAryl)_6$ complexes [51]. The lowest excited states of $Cr(CNAryl)_6$ has a Cr→ArNC MLCT

character. However, no Cr–C antibonding orbitals are populated [99]. A vibronic interaction with higher LF states is therefore required. It may also be speculated that relatively low-lying M→CO MLCT excited states occur even in substituted carbonyls of the type $M(CO)_4L_2$ or $M(CO)_5L$; L = Lewis base ligand; M = Cr, Mo, W. For L_2 = α-diimine, these states lie above the M→diimine MLCT states but below the metal-localised LF states. Validity of this hypothesis and possible photochemical implications still have to be tested experimentally. However, it is interesting to note that the CO stretching frequencies of $W(CO)_5(py)$ in its lowest excited state are lower compared with the ground state, implying an increase of the electron density in the π*(CO) orbitals on excitation [100]. It is difficult to reconcile this observation with the presumed ^{3}LF character of this excited state. On the other hand, such an effect could arise from a W→CO MLCT excitation.

A CO photodissociation from $Ni(CO)_4$ has to occur from Ni→CO MLCT excited states since no LF states are available. Indeed, the CASSCF/CASPT2 calculation has predicted a group of low-lying Ni→CO MLCT states derived from the excitations into the t_2-π*(CO) orbital [57]. It would be interesting to examine the shape of the MLCT potential energy surfaces since it is not obvious how the MLCT excitation can cause a CO dissociation in the absence of LF states. A weakening of the Ni–CO π back-bonding and/or a vibronic mixing with σ-antibonding states derived from 3d→4s Ni-centred excitations are plausible explanations.

3.3. Homolysis of a metal–ligand bond

An introduction of an alkyl or metallic ligand to the axial position of MLCT-active diimine–carbonyl complexes has a dramatic effect on their photochemical reactivity. This is, for example, the case of the complexes:

fac-Re(E)$(CO)_3$(diimine); E = $SnPh_3$, $Mn(CO)_5$, $Re(CO)_5$, benzyl (Bz), Et, ^{i}Pr [60–64,101–103]

fac-Mn(E)$(CO)_3$(diimine); E = Bz, ^{i}Pr; $Mn(CO)_5$ [56,101–103]

cis(*CO,CO*),*trans*(*E,E'*)–Ru(E)(E')$(CO)_2$(diimine); E = ^{i}Pr, $SnPh_3$, $GePh_3$, $Mn(CO)_5$, $Re(CO)_5$, E' = alkyl or another metallic ligand but not a halide [64,104–106]

Irradiation into their lowest absorption band often causes a very efficient[2] homolysis of the M–E bond, producing free radicals:

$$M(E)(CO)_3(diimine) \xrightarrow{h\nu} M(S)(CO)_3(diimine)^\bullet + E^\bullet \quad (2)$$

M = Mn, Re

$$Ru(E)(E')(CO)_2(diimine) \xrightarrow{h\nu} Ru(S)(E')(CO)_2(diimine)^\bullet + E^\bullet \quad (3)$$

All the experimental evidence, which was extensively reviewed elsewhere [59,90], clearly shows that the M–E bond homolysis is the primary photochemical step.

[2] Complexes containing the Ph_3Sn ligand are only a little reactive, presumably due to an exceptional strength of M–Sn bonds.

Moreover, a nanosecond FT–EPR study has demonstrated conclusively [64] that these homolytic reactions occur from a spin-triplet excited state. The quantum yields usually approach unity and are independent of the temperature and excitation wavelength. The reaction rate and actual mechanism are very dependent on the structure of the reactive molecule and the solvent. Thus, reactions of most of the Ru complexes and of those Re complexes which contain the bpy′ ligand occur very rapidly, apparently from a Franck–Condon excited state. A lifetime of ca. 800 fs has been estimated for the homolysis of the Re–C(Et) bond in $Re(Et)(CO)_3(bpy')$ [107]. On the other hand, the photochemical homolysis of a Re–C(Bz) bond in $Re(Bz)(CO)_3(^iPrDAB)$ in a noncoordinating, nonpolar, hydrocarbon solvent takes place from a relaxed, thermally equilibrated, excited state with a lifetime of 250 ns. The reaction is at least 104-times faster in coordinating and/or polar solvent like THF [61,62]. Complexes $Re(E)(CO)_3(^iPr–DAB)$ in which E = Et, ^{i}Pr or a metal-fragment behave similarly [62,63].

From a mechanistic point of view, it is now interesting to ask about the nature of the reactive excited state and the role, if any, of MLCT excited states in the photochemical metal–ligand bond homolysis. Alkyl or metallic ligands are bound to the central metal atom covalently, utilising their energetically high-lying, occupied, σ-bonding orbital. The reactive state involves an electron excitation from a M–E σ-bonding orbital to the π^*(diimine) orbital [6,7,59,90,101]. These states are usually denoted $\sigma\pi^*$ or SBLCT (sigma bond-to-ligand charge-transfer). They are distinct from MLCT states since, at least in their pure form, no depopulation of metal d_π orbitals takes place. The actual change of the electron density on the central metal atom depends on the contribution of the metal nd_{z^2} and $(n+1)p_z$ characters to the M–E σ-orbital. Time resolved IR spectra have indicated only a very small decrease or even a minute increase in the metal-localised electron density in the $3\sigma\pi^*$ state of $Re(Bz)(CO)_3(^iPr–DAB)$ and $Ru(SnPh_3)_2(CO)_2(^iPr–DAB)$, respectively [61,62,108]. Interestingly, the bond homolysis seems to be the most important deactivation pathway of $3\sigma\pi^*$ excited states. If this reaction was prevented in a low-temperature glass, the $3\sigma\pi^*$ states are often long-lived and emissive. The shapes of the potential energy surfaces of $3\sigma\pi^*$ states and, hence, their reactivity seem to be strongly dependent on the molecular structure and the medium.

It remains to be discussed what is the nature of the initial optically excited state of the complexes which undergo photochemical bond homolysis and how is the $3\sigma\pi^*$ state populated. Based on resonance Raman spectroscopic data, the lowest visible absorption band of reactive Re and Mn complexes has been attributed to a MLCT transition [6,109]. Moreover, it was argued that the $\sigma \rightarrow \pi^*$ electronic transition is overlap-forbidden and, hence, spectroscopically rather weak. It was therefore concluded [6,7] that irradiation with visible light initially excites the molecule to a ^{1}MLCT state from which the reactive $3\sigma\pi^*$ state is populated nonradiatively. This may well be the case of the photoreactive $Mn(E)(CO)_3$(diimine) complexes. A CASSCF/CASPT2 calculation on the $Mn(H)(CO)_3$(H–DAB) model have shown an avoided crossing between the potential energy curves of the (Mn → DAB) 1MLCT and the $3\sigma_{MnH}\pi^*$ states at a slightly

elongated Mn–H distance [77,78,110]. These two states are spin–orbit and non-adiabatically coupled. A calculation of the wavepacket dynamic has shown that the Mn–H bond can undergo a low-probability photochemical Mn–H bond homolysis, despite the fact that the $3\sigma\pi^*$ state lies more then 8000 cm − 1 above the MLCT one at the geometry of the Franck–Condon excitation. Replacing H by an alkyl ligand causes a strong mixing between the 3MLCT and $3\sigma\pi^*$ states while the Franck Condon state retains its 1MLCT character [88,110]. For the Et axial ligand, all the potentially reactive spin-triplet states with a significant $\sigma\pi^*$ contribution occur below the initially excited 1MLCT state and an efficient Mn–Et bond homolysis is predicted, in accord with experiments.

The nature of the optically excited state is probably somewhat different in the case of complexes of heavier metal atoms, Re or Ru. Calculations on the $Re(H)(CO)_3(H\text{–}DAB)$ model [88,110] have revealed an extensive mixing between the MLCT and $\sigma\pi^*$ characters already in the Franck–Condon, spin-singlet, excited state. The interaction between the $6p_z(Re)$ and π^* orbitals removes the overlap restrictions on the intensity of the $\sigma \rightarrow \pi^*$ spectroscopic transition. This $\sigma\text{–}\pi^*$ interaction is clearly evidenced already by ground-state spectroscopic properties of the $Ru(E)(E')(CO)_2$(diimine) complexes [108,111,112] and by a surprisingly large Sn hyperfine splitting constant observed in the EPR spectrum of the $[Ru(SnPh_3)_2(CO)_2(^iPr\text{–}DAB)]^{\bullet -}$ radical-anion [112]. It thus appears that the $Re(E)(CO)_3$(diimine) and $Ru(E)(E')(CO)_2$(diimine) complexes are optically excited into a mixed $1MLCT/\sigma\pi^*$ state from which the reactive spin-triplet state is easily populated due to a large Re spin–orbit coupling. This is in accord with the observation that the $Re(S)(CO)_3(bpy')^{\bullet}$ radicals are formed promptly, in about 800 fs after the excitation of the $Re(Et)(CO)_3(bpy')$ complex [107]. The extent of the $MLCT/\sigma\pi^*$ mixing is different for the singlet and triplet states [88,110]. It may also depend on the nature of the diimine and E ligands and on the solvent. The variable extent of the $MLCT/\sigma\pi^*$ mixing in the reactive spin-triplet state, together with the changing relative energetic position of the optically excited and reactive states, could possibly account for the wide time scale, fs–μs, of photochemical metal–ligand bond homolysis reactions, vide supra.

The photochemical reactivity of $Re(Me)(CO)_3$(diimine) complexes is rather exceptional. A relatively inefficient Re–Me bond homolysis was found for diimine = bpy', ^{i}Pr–PyCa or ^{i}Pr–DAB [60,61,113]. The temperature and/or excitation energy dependence of the quantum yield indicate a barrier on the potential energy surface of the optically excited, presumably MLCT, state due to an avoided crossing with the $3\sigma\pi^*$ state. This barrier may be partly overcome during the propagation from the Franck–Condon excited state. The rest of the excited molecules rapidly relax to an unreactive state of a ^{3}MLCT or mixed $^3MLCT/\sigma\pi^*$ character. This mechanism is supported by the results of a femtosecond spectroscopic study of $Re(Me)(CO)_3(bpy)$ which has shown that both the photoproduct and the relaxed state are formed independently of each other within 800 fs [107]. Interestingly, this behaviour resembles the CO dissociation from $Cr(CO)_4(bpy)$ described above. The general picture shown in Fig. 5a may be applied, with a $3\sigma\pi^*$ state in place of the ^{1}LF one.

Finally, it should be noted that the photochemical bond homolysis has been observed also for complexes which do not contain an oxidisable metal atom and, hence, do not possess MLCT states. This is, for example, the case of $Pt(Me)_4(C_6H_{11}-DAB)$ [114,115] or $Zn(R)_2(t$Bu-DAB) [116]. Their reactive $3\sigma\pi^*$ state is populated after an optical excitation into a $1(\sigma \rightarrow \pi^*)$ transition, which, for these species, is spectroscopically allowed. Obviously, it is the $3\sigma\pi^*$ state that is essential for the homolytic reaction, not the MLCT one. However, if both MLCT and $3\sigma\pi^*$ states are present, as for the compounds discussed above, an interesting state mixing and coupled MLCT/$3\sigma\pi^*$ dynamics takes place.

4. Reactions of relaxed MLCT excited states

Although the prompt reactivity of Franck–Condon MLCT excited states discussed in the previous section is mechanistically very interesting, it does not represent the most common type of MLCT photochemistry. Excitation of MLCT transitions of many complexes, especially of heavier transition metals, is followed only by a vibrational and electronic relaxation. A thermally equilibrated ^{3}MLCT excited state is formed. Its lifetime is often long enough to allow for further chemical reactions of the excited molecule, in addition to its nonradiative and radiative decay to the ground state. Unlike prompt reactions, the chemical reactions of relaxed excited states may be described in terms of conventional reaction kinetics and transition state theory. The high reactivity of relaxed excited states may essentially be attributed to their higher energy and redistributed electron density, as compared with the ground state.

4.1. Thermodynamic activation

Population of a long-lived, inherently stable, MLCT excited state activates the molecule thermodynamically by increasing its energy content. Such an excited molecule could be involved in a host of energy- or electron-transfer reactions. Most of MLCT-active complexes are also redox-active, able to undergo fast and chemically reversible oxidations and/or reductions. This combination of a ground-state redox-activity with the existence of long-lived excited states makes the MLCT-active molecules prone to photochemical electron transfer reactions. Optical excitation activates such molecules thermodynamically by changing their redox potentials E^0. Reactivity is then mostly determined by the extra excitation energy E_{00} which makes them much stronger reductants and/or oxidants than corresponding ground state molecules:

$$E^0(A+/A^*) = E^0(A+/A^*) - E_{00} \quad (4)$$

$$E^0(^*A/A-) = E^0(A/A-) + E_{00} \quad (5)$$

where A and *A stand for the ground and excited state, respectively. Very simply, it may be said that the MLCT excitation simultaneously creates within the molecule

a strongly reducing and oxidising site, the reduced ligand and oxidised metal atom, respectively. This behaviour is shown, for example, by many RuII, OsII, ReI, CuI or PtII complexes containing α,α'-diimine ligands. Electron-transfer reactivity of MLCT-active complexes has been the subject of many excellent reviews, see e.g. [3,117–120]. For a more recent work on CuI and PtII complexes see, e.g. [121,122], respectively, and references therein.

4.2. Associative reactivity of MLCT states

The simple charge-separated formulation described by the Eq. (1) applies well to relaxed charge-transfer excited states. Their chemical properties may be discussed in terms of the reactivity of the oxidised metal atom or the reduced ligand which could become strongly nucleophilic or electrophilic, respectively, in a MLCT state. Accordingly, photochemical associative ligand substitutions, oxidative additions and ligand protonations were observed for MLCT excited states of organometallic complexes of heavier metal atoms.

4.2.1. Ligand substitution

The photochemistry of $M(CO)_4(phen)$ complexes; M = Mo, W; represents a prototypical case of an associative CO substitution from a MLCT state, Fig. 8. Visible irradiation of their solutions containing a large excess of a Lewis base L (phosphines, phosphites, amines, etc.) results in a photosubstitution of the axial CO ligand, producing *fac*-$M(CO)_3(L)(phen)$. Quantum yields are low, usually in the range $10-6-10-2$. They are strongly dependent on the chemical nature of the incoming ligand L [42,43,46]. For L = phosphine or phosphite, the quantum yields decrease with an increasing cone angle [42,46]. A deep insight into the mechanism of these associative photochemical substitutions emerged from the studies of combined dependencies of the quantum yield on the pressure, ligand concentration and excitation wavelength [44,46]. Essentially, it was found that the reactivity observed under irradiation into the visible MLCT absorption band consists of parallel dissociative and associative pathways. The prompt CO dissociation from the Franck–Condon MLCT state seems to be responsible for the dissociative route. For Mo, the quantum yield of the dissociative reaction is about 100 times smaller than for Cr [45]. A further, ca. 1000-fold decrease occurs on going from Mo to W [46]. The associative pathway is important for both Mo and W, but negligible or even absent for Cr. The change of the mechanism is clearly demonstrated by the

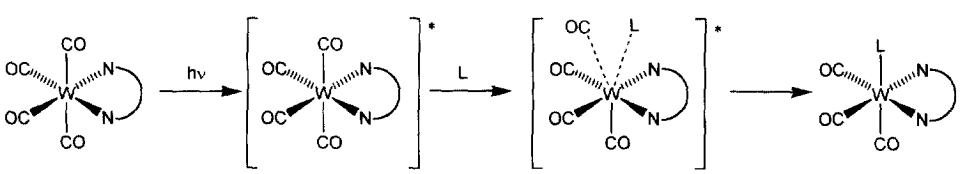

Fig. 8. Associative photochemical substitution of $W(CO)_4(bpy)$.

volume of activation whose values change from $+2.1$ cm^3 mol^{-1} for Cr [45] to -10.7 or -9.6 cm^3 mol^{-1} for Mo or W, respectively [46], as measured for the reaction with PMe_3, under 546 nm irradiation.[3] The quantum yield of the associative pathway increases rapidly with increasing ligand concentration [46]. The very presence of two parallel/competitive reaction pathways, rate of each being differently dependent on reaction conditions, gives rise to complicated dependencies of the overall photosubstitution quantum yield on the external pressure or excitation energy [43,46,47]. Moreover, different dependencies were obtained for different incoming ligands and their concentrations. Thus, for example, a rather unusual increase of the overall quantum yield with decreasing excitation energy (increasing wavelength) have been observed for some photosubstitution reactions of $W(CO)_4$(phen) [43].

In summary, a complete changeover of the mechanism of the MLCT-induced photosubstitution from dissociative to associative have been observed on going from $Cr(CO)_4$(phen) to $Mo(CO)_4$(phen) and, especially, $W(CO)_4$(phen). A relatively inefficient dissociative component still contributes to the reactions of the Mo complex, becoming very small for W. The associative reaction is most efficient for sterically undemanding incoming ligands at high concentrations and under irradiation into the low-energy part of the MLCT absorption band. For example, CO photosubstitution in $M(CO)_4$(phen); M = Mo, W; by PMe_3 follows an entirely associative pathway when irradiation wavelengths longer than 436 nm were used [46]. The MLCT photosubstitution reactions of other $W(CO)_4$(diimine) complexes; diimine = phen derivatives, bpy, R–DAB; are also associative [42]. Interestingly, the photosubstitution quantum yields of $W(CO)_4$(phen) and $W(CO)_4$(phen–NO_2) are comparable [26], indicating that the associative pathway is activated by the virtual oxidation of the W atom in the MLCT state, regardless the site of the predominant localisation of the excited electron, N(phen) donor atoms and $-NO_2$ group, respectively.

A changeover from a dissociative to associative mechanism on going from Cr to Mo and W was also observed for the photochemical substitution of the CNAryl ligand in $M(CNAryl)_6$ complexes by pyridine [48,49]. Quantum yields of this reaction decrease with increasing bulkiness of the aryl substituent in the case of the associatively reacting Mo and W complexes. No steric effect was found for the photodissociative Cr species. An associative photochemical substitution was also reported for the MLCT-active dinuclear complex $(CO)_4Mo(\mu\text{-PMD})_2Mo(CO)_4$ [123,124]. An unusual associative photosubstitution of a bromide ligand by $P(^nBu)_3$ was found [125] to take place on MLCT excitation of $Re(Br)(CO)_3$(DTO); DTO = *N*,*N*′-dimethylpiperazine-2,3-dithione.

The effect of the metal atom on the photosubstitution mechanism is indeed intriguing. It is caused by two simultaneous trends: a decrease of the efficiency of

[3] It is interesting to note that the dissociative component becomes much more important under UV irradiation into higher MLCT and LF transitions. For example, activation volumes of $+1.5$ and $+3.2$ cm^3 mol^{-1} were measured for the photochemical reaction of $W(CO)_4$(phen) with PMe_3 at 336 and 313 nm, respectively [46].

the prompt dissociation in the order Cr > Mo ≫ W and the appearance of the associative pathway for Mo and W. The former trend could be explained by the fact that M–CO bonds are stronger and LF states more energetic for W than Cr. The avoided crossing between ^{1}MLCT and LF potential energy curves (Fig. 5) thus occurs at much longer distances for W than Cr. Hence, the potential well on the initially excited ^{1}MLCT surface of W complexes is deeper. The vibrational/electronic relaxation of the Franck–Condon state to a ^{3}MLCT state occurs preferentially to the CO dissociation, being aided by larger spin–orbit coupling. The associative MLCT photosubstitution is made possible by three factors: (i) virtual oxidation of the metal atom in the MLCT state which makes it electrophilic, (ii) large size of Mo and W atoms which makes them accessible to the nucleophiles, and (iii) excited state lifetime long enough to allow for a bimolecular reaction. The size effect on the substitution mechanism is well know also for thermal organometallic reactions. The lifetime of the relaxed ^{3}MLCT states indeed increases in the order Cr ≪ Mo < W. Thus, lifetimes of 90 ps and ca. 5 ns were observed for the ^{3}MLCT state of $Cr(CO)_4$(bpy) [83] and $W(CO)_4$(phen) [43], respectively. Similarly, the relaxed ^{3}MLCT states of the Mo and W isonitrile complexes $M(CNIph)_6$; Iph = 2,6-diisopropylphenyl; are relatively long-lived, 43 and 83 ns, respectively [48]. On the other hand, no excited state was detected for $Cr(CNIph)_6$ or $Cr(CNPh)_6$, even on a picosecond timescale [50]. Finally, it should be noted that associative substitutions of complexes in a ^{3}MLCT state are formally spin-forbidden since the products are formed in their spin-singlet ground states. However, the large spin–orbit coupling of Mo or W apparently allows for a fast intersystem crossing to the ground state, most probably at the stage of the seven-coordinate intermediate.

4.2.2. Oxidative additions

Photochemical oxidative additions represent another type of associative reactions of relaxed ^{3}MLCT states. They are known for complexes of oxidisable metal atoms which can increase their coordination number to yield stable products. The presence of a metal-localised unpaired electron in a relaxed ^{3}MLCT state leads to a radical-like primary photochemical step. An atom-abstraction is thus a typical photochemical reaction of MLCT-active coordinatively unsaturated complexes.

For example, the ^{3}MLCT excited state of $Pt^{II}(Me)_2$(phen) reacts with ^{i}PrI to yield $Pt^{III}(I)(Me)_2$(phen) as the primary product [68]. This photoreaction initiates a radical chain process which leads to $Pt^{IV}(I)_2(Me)_2$(phen) and PtIV(I)(^{i}Pr)$(Me)_2$-(phen) final products [68]. Similarly, the long-lived (2.4 μs) ^{3}MLCT excited state of $Pt^{II}(thpy)_2$; thpy = deprotonated 2-(2-thienyl)pyridine; reacts with CH_2Cl_2 or $CHCl_3$ producing $Pt^{IV}(Cl)(R)(thpy)_2$; R = CH_2Cl or $CHCl_2$; respectively [69,126]. A detailed study [69] of the effects of the excitation wavelength and triplet quenchers on the quantum yield has shown that the primary Cl atom abstraction occurs by several pathways. Besides the bimolecular reaction between the relaxed ^{3}MLCT state and CH_2Cl_2 or $CHCl_3$, the reaction may also occur directly from the Franck–Condon excited ^{1}MLCT state and, at higher excitation energies, even from an intraligand state. The latter two prompt reactions involve a propagation from

the initially excited states onto the potential energy surface of a charge-transfer to solvent state, CTTS, that can be approximately formulated as $[Pt^{III}(thpy)_2^+][S^-]$; $S = CH_2Cl_2$ or $CHCl_3$. (Note that the occurrence of this process is not limited by the excited state lifetime since the reactive solvent molecules are weakly interacting with the photoactive molecule already at the instant of the excitation.) Photochemical oxidative additions are not restricted to planar complexes. Irradiation of octahedral complexes $M^0(CNPh)_6$; M = Mo, W; in $CHCl_3$ leads to stable seven-coordinated $[M^{II}(CNPh)_6(Cl)]^+$ products. Quantum yields are high, 0.28 (W) and 0.11 (Mo) [48,49].

Several interesting photocatalytic reactions involve an oxidative addition as the primary photochemical step. This is the case of *trans*-$Rh(PMe_3)_2(CO)(Cl)$ which undergoes a photochemical oxidative addition of a benzene C–H bond [71–73]. Two stereoisomers of $Rh(PMe_3)_2(CO)(Cl)(Ph)(H)$ are the primary photochemical products [72]. The nature of the reactive excited state is not known. However, it seems likely that a Rh→CO or Rh→PMe_3 MLCT state is responsible. Such a photochemical oxidative addition of a C–H bond is the crucial step of the carbonylation of alkanes, aromatic hydrocarbons, or derivatives of thiophene photocatalysed by $Rh(PMe_3)_2(CO)(Cl)$ [71,72,127,128]. Another example of a catalytically important associative excited state redox reaction is provided by the photocatalysis of the water gas shift reaction by $[Cp^*Ir(phen)(Cl)]^+$ [129–131]. The hydrido complex $[Cp^*Ir(phen)(H)]+$ was identified as the photoactive species. It has a long-lived (190 ns) excited state presumably of a MLCT origin [132]. The excited $[Cp^*Ir(phen)(H)]+$ complex reacts with water producing H_2 and, in the presence of Cl^- ions, regenerating the $[Cp^*Ir(phen)(Cl)]^+$ catalyst. The photochemical step thus closes the catalytic cycle and releases one of the products, H_2. The mechanism of the photochemical H_2 evolution has not been studied in detail.

4.2.3. Ligand-localised reactions

The acceptor ligand is virtually reduced by one electron in a relaxed 3MLCT excited state, see Eq. (1). Hence, a ligand-localised nucleophilic or radical-type photoreactivity may be expected. In reality, complexes with sufficiently long-lived MLCT states usually contain diimine ligands, namely polypyridyls or polyazines. The excited electron is largely delocalised in an extensive π system and its chemical effects are rather limited. The virtual ligand reduction is best manifested by proton-transfer reactions of MLCT excited states of those complexes which contain acceptor ligands with acidic or basic sites. MLCT excitation strongly affects their pK_a values. The conjugated bases become more basic in a MLCT state and the kinetics of the deprotonation of the conjugated acids is affected as well. This is, for example, the case of polypyridyl ligands bearing the –COOH or –OH substituent or polyazine ligands with uncoordinated nitrogen atoms, for instance 2,2-bipyrimidine or 2,2′-bipyrazine [133–137]. An interesting ligand-centred photochemical oxidative addition occurs on irradiation of the carbyne complexes $Os(CPh)(CO)(PPh_3)_2(Cl)$ or $[Os(CPh)_2(CO)(PPh_3)_2]^+$ in solutions containing HCl. Apparently, the primary photochemical step involves protonation of the carbon donor atom of the carbyne ligand that becomes nucleophilic in the Os→CPh MLCT excited state [138].

5. Delayed dissociative ligand substitution through a relaxed MLCT excited state

The complexes $W(CO)_5(py–X)$ show dissociative photosubstitution reactions whose mechanism is, however, very different from the prompt ligand dissociations discussed in Section 3. The nature of the lowest excited state of these molecules is determined by the substituent X at the 4-position of the pyridine ring: complexes of electron-accepting py–X ligands; X = CN, formyl, acetyl or benzoyl; have a $W \rightarrow py–X$ MLCT lowest excited state while a LF state is the lowest one for X = H or Me [1,33,139,140]. This is clearly manifested by the absorption spectra. The LF band always occurs at ca. 400 nm. The absorption band due to the MLCT transition lies at higher energies, in the UV region, for X = H or Me, shifting to longer wavelengths, below the LF band, for complexes with electron-withdrawing substituents X. Only those complexes whose lowest excited state has a MLCT character show a long-lived emission in fluid hydrocarbon solutions at room temperature. Lifetimes range from 200 to 500 ns, depending on X and the solvent [34,35]. Evidently, a relaxed, thermally equilibrated, ^{3}MLCT excited state is populated. Regardless the substituent X and, hence, the nature of the lowest excited state, irradiation into the lowest absorption band results in a substitution of the py–X ligand:

$$W(CO)_5(py–X) \xrightarrow{h\nu} W(CO)_5(S) + py–X \quad (6)$$

The quantum yield drops from 0.5–0.8 to ca. 0.02 on going from the complexes whose lowest absorption band belongs to a LF transition (X = H, Me) to those with a lowest MLCT band (X = CN, acetyl, etc.) [33]. The dissociative character of the reaction in Eq. (5) has been demonstrated by the positive values of the activation volume [35] and by the observation that the of the solvated photoproduct $W(CO)_5(S)$ is formed even in noncoordinating methylcyclohexane [36] or *n*-heptane [37] solvents, both under the visible or UV excitation.

Quenching and, especially, time-resolved IR spectroscopic experiments have proven that the low-yield photosubstitution induced by a visible-light irradiation into the MLCT absorption band of $W(CO)_5(py–X)$; X = CN or acetyl; occurs only after a relaxed ^{3}MLCT state was formed [34,36,37,141]. The photosubstitution mechanism is shown schematically in Fig. 9. The optical MLCT excitation is followed by a vibrational/electronic relaxation that produces a thermally equilibrated ^{3}MLCT excited state within ca. 40 ps after the excitation [142]. The ^{3}MLCT state then undergoes two parallel processes which take a few hundreds of nanoseconds: a decay to the ground state and a thermal population of the higher-lying ^{3}LF state from which the py–X ligand dissociates rapidly and the $W(CO)_5(S)$ photoproduct is formed. This picture agrees well with the experimental data: (i) regardless the excitation wavelength and nature of the py–X ligand, it is always the weakest skeletal bond in the molecule, W–N, that dissociates. This reaction is exactly the one expected for the lowest LF state of a $d(\pi) \rightarrow d(\sigma^*_{WN})$ origin. (ii) The quantum yield is large and temperature-independent for complexes with the lowest LF state, populated directly by an optical excitation. On the other hand, the quantum yield is much smaller for complexes with the lowest MLCT state since it is determined by

the efficiency of the population of the LF state. (iii) The yield and rate of the substitution reaction of the complexes with a lowest MLCT state is temperature-dependent. Rather large activation energies, 2500–4000 cm^{-1}, were measured and attributed to the ^{3}LF–3MLCT energy gap [34,36,37], vide infra. (iv) Positive volume changes, +4.3 and +1.8 $cm^3\ mol^{-1}$ were determined [35] for the population of the LF state from the MLCT one. This agrees with the expected molecular expansion caused by the population of the σ-antibonding d orbital in the LF state. (v) The quantum yield is still quite high, ca. 0.1, even for complexes with a lowest MLCT state, when irradiated in the UV into the higher LF band [33]. Apparently, the ^{1,3}MLCT states are mostly bypassed during the relaxation of the optically excited higher ^{1}LF state which is either dissociative itself or decays through the reactive ^{3}LF state, see Fig. 9.

Relatively slow, low-yield, dissociative substitution of an acceptor ligand from a relaxed ^{3}MLCT state was found also for other complexes of the second-row transition metals which possess relatively close lying MLCT and LF states. This is the case of photosubstitution reactions of $[Ru(NH_3)_5(py–X)]^{2+}$ complexes [22–24,28] whose quantum yields depend on experimental conditions in the same way as those of $W(CO)_5(py–X)$. Analogous $[Fe(CN)_5(py–X)]^{3-}$ complexes, whose LF states are pushed above the MLCT ones by the strong-field CN ligands, behave

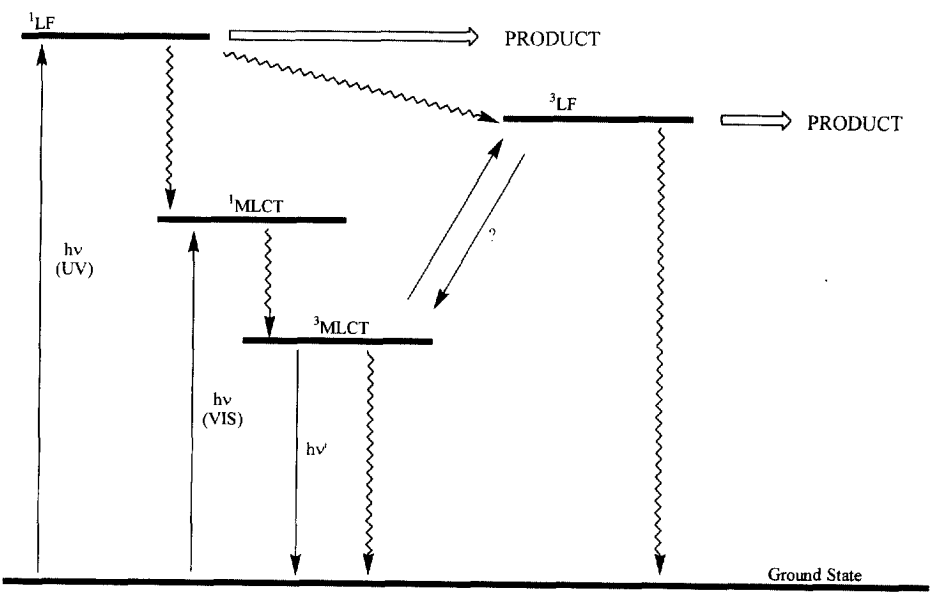

Fig. 9. State (Jablonski) diagram describing the mechanism of the delayed ligand photosubstitution of $W(CO)_5(py–X)$ and related complexes. Irradiation with the visible light, $h\nu$(VIS), excites the GS→ ^{1}MLCT transition. The ^{1}MLCT state relaxes to the long-lived ^{3}MLCT state, from which the reactive ^{3}LF state is populated thermally. This may occur either as an irreversible nonradiative transition or as a dynamic equilibrium. Irradiation with the UV light, $h\nu$(UV), excites the GS→ ^{1}LF transition. The ^{1}LF state undergoes a ligand dissociation and/or it relaxes to the reactive ^{3}LF state.

similarly [143]. Photosubstitution of a py–X ligand in $W(CO)_4(py–X)_2$ is another example [144].

The photochemical substitution of a polypyridyl ligand in $Ru(bpy)_3 2+$ and related complexes also proceeds from a higher LF state that is thermally populated from a long lived, relaxed, ^{3}MLCT state [8,29–32,145–147]. This reaction was studied in a great detail since it limits the use of Ru^{II}–polypyridyls as photosensitisers in light-energy conversion processes. The activation energies are rather high, ranging from 3000 to 5000 cm^{-1}. The energy difference between the LF and MLCT states and, hence, the photochemical activation energy and photosubstitution quantum yield may be tuned by a judicious choice of the ligands. Thus, strong-field ligands rise the energy of the LF states while those with low-lying π^*-acceptor orbitals diminish the energy of the MLCT state. A combination of these two effects allows to design photostable Ru^{II}–polypyridyl complexes, suitable as photochemical sensitisers. The Os^{II}–polypyridyl complexes are much more photostable than their Ru counterparts since the osmium LF states lie at higher energies.

The photochemical activation energy observed for delayed reactions may be interpreted in two ways, depending on the character of the conversion between the ^{3}MLCT and ^{3}LF states, see Fig. 10. For complexes in which the ^{3}LF state dissociates relatively slowly and the ^{3}LF potential energy surface has a bound shape, a dynamic equilibrium between the ^{3}MLCT and ^{3}LF states may exist. The corresponding equilibrium constant is then determined by the ^{3}LF–^{3}MLCT energy gap, according to Boltzmann statistics. The experimental photochemical activation energy then measures this energy gap, ΔE. On the other hand, if the LF state were completely dissociative, the transition from the ^{3}MLCT to the ^{3}LF state would occur as an irreversible surfaces crossing. The experimental photochemical activation energy would then have the meaning of the true activation energy E_a, that is of the energy difference between the crossing point of the ^{3}MLCT and ^{3}LF curves and the minimum on the ^{3}MLCT surface. It is difficult to distinguish between these possibilities experimentally. Most of the work published so far prefers the interpretation based on a dynamic $^3\text{MLCT} \rightleftharpoons {}^3\text{LF}$ equilibrium. However, given the known ultrafast reactivity of ^{3}LF states, an irreversible nonradiative transition to a dissociative ^{3}LF state, followed by a much faster dissociation, seems to be a more likely mechanism, especially for organometallic compounds.

Finally, it should be noted that a similar mechanism involving a thermal population of a dissociative $^3\sigma\sigma^*$ state from a relaxed, long-lived, $^3\sigma\pi^*$ state seems to be responsible for a Ru–Sn bond homolysis in $Ru(SnPh_3)_2(CO)_2(^i\text{Pr–DAB})$ [104].

6. MLCT reactivity: structural relations, implications, and possible applications

Broadly speaking, there are three ways how a MLCT excitation can activate molecules of organometallic or coordination compounds toward photochemical reactions in which bonds are broken or formed: (i) prompt reactions from the

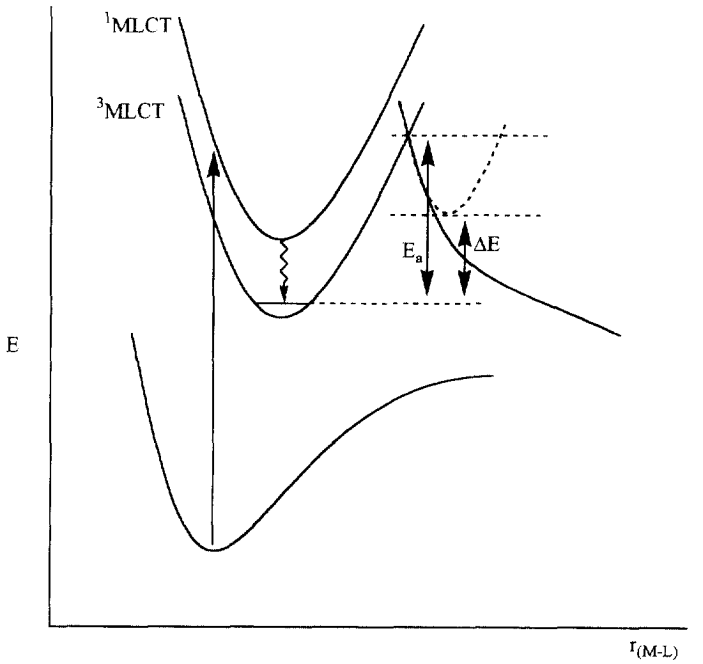

Fig. 10. Two possible interpretations of an apparent activation energy of a delayed photochemical reaction. Irreversible transition from a long-lived ^{3}MLCT state to a dissociative ^{3}LF state (full-line hyperbola) occurs with a measurable activation energy, E_a. On the other hand, if a ^{3}MLCT $\rightleftharpoons$ ^{3}LF equilibrium exists (^{3}LF = dashed parabola), an energy difference between the two states is measured, ΔE_a.

optically excited MLCT state, (ii) associative reactions of a long-lived, relaxed ^{3}MLCT state, and (iii) a thermal population of a different, but reactive, excited state from a relaxed ^{3}MLCT state. In addition, a population of a long-lived ^{3}MLCT state activates molecules in a thermodynamic sense by changing their redox potential. In any case, high oscillator strengths of MLCT transitions ensure a fast and efficient absorption of incident light. Hence, irradiation into MLCT absorption bands is a very convenient way to run a photochemical reaction, whatever the actual mechanism is. This is, among others, one of the reasons for a wide use of MLCT-active complexes as sensitisers of light-energy conversion or in light-harvesting supramolecular antenna systems. MLCT states can be even prepared by a two-photon excitation using red light [148]. This could lead to entirely new biological, medical or material applications. The detailed mechanisms and kinetics of MLCT photochemistry are still far from understood. However, some general relations are already emerging from a combination of recent experimental and theoretical research.

Prompt photochemical reactions take place on a femtosecond timescale, directly from the Franck–Condon excited state. Their quantum yields are dependent on excitation energy varied within the spectral range of the MLCT absorption band.

They may also be temperature-dependent, but not necessarily. Activation energies are expected to be smaller than about 1500 cm^{-1}. The simple one-electron view of MLCT excited states, based on the bonding and antibonding characters of the orbitals depopulated and populated on excitation, is largely irrelevant to the mechanism of the prompt dissociation. Its understanding requires to work on the level of potential energy surfaces of several states. The character of the reactive excited state, that is its orbital parentage, changes gradually along the reaction coordinate. The quantum yield, rate and selectivity of a prompt reaction are thus largely determined by the shape of the potential energy surface of the optically excited ^{1}MLCT state, see Fig. 5. It depends on the bonding properties of the MLCT state and on its interactions with other excited states along possible reaction and/or relaxation coordinates (pathways). A qualitative insight may be obtained from considerations of accompanying orbital energy changes. Further information about the direction of the initial bond weakening from the Franck–Condon excited state may be obtained by examining possible vibronic interactions between the MLCT and higher lying, potentially dissociative, states [40]. Their symmetries allow to determine the symmetry of the vibration activated by the Franck–Condon excitation and, hence, of the reaction coordinate. More accurate insight is, however, obtained from quantum chemical calculations of the potential energy surfaces [58,77,78,81,88,110]. Their knowledge allows to describe the short-time excited state dynamics as a wavepacket propagation [74–77]. Hopefully, it will soon be possible to draw some general conclusions from a series of calculations performed on sets of representative photoreactive molecules. An inclusion of solute-solvent interactions will be a major step toward a realistic theoretical description of a prompt MLCT reactivity.

Generally, a prompt reactivity is expected for those MLCT excited states whose potential energy curve along the reaction coordinate is (nearly) dissociative with only a small energy barrier or no barrier at all. This requires that the energy of the higher dissociative (LF or $\sigma\pi^*$) state falls very steeply as the length of the dissociating bond increases. Such a situation arises especially for complexes of the metals from the first and, to a lesser extent, second transition row whose bonding interactions are rather short-range, especially with the CO ligand. In a homologous series of similar complexes, the efficiency of the prompt ligand dissociation generally decreases with decreasing energy of the π^* orbital of the acceptor ligand. Resulting low-lying MLCT states shows a deep energy minimum at only a little distorted geometry. The Franck–Condon excitation then falls into this energy well, too much below the barrier. However, the reaction may still occur due to a resonance coupling with states of a dissociation continuum [76,81,89], should the topology of the ground and excited state potential energy surfaces permit, see Fig. 7.

So far, the prompt mechanism has been established for a photochemical dissociation of M–CO and M–CNAryl bonds and for a homolysis of M–alkyl or metal–metal bonds, vide supra. Probably, it is also involved in the photodissociation of other ligands, namely olefins, from complexes of low-valent metal atoms. Moreover, it is quite possible that the MLCT potential energy surfaces may be

coupled to surfaces of reactive excited states other than LF or $\sigma\pi^*$. For example, ligand (olefin) isomerisation or solvent reduction are known to take place on MLCT excitation [1,9,21,24]. Although no mechanistic details have been reported, these reactions probably involve a propagation on an initially excited MLCT potential energy surface that is, however, coupled with an intraligand or a CTTS excited state, respectively, along the reaction coordinate. Ultrafast intramolecular electron transfer reactions which involve coupling of an initially populated MLCT state to a different MLCT or LLCT[4] state [90] or to a conduction band of a semiconductor [149–152] are also known.

Experimental and theoretical investigations of prompt MLCT reactions are very important for the fundamental understanding of the short-time dynamics of excited states and chemical bonds. Prompt MLCT reactivity defies not only the simple one-electron view of MLCT excitation but also the common description of photochemical reactivity in terms of a cascade of temporally distinct steps. Traditionally, the reactive, nonradiative, and radiative decay pathways and conversions between excited states are described using a state (Jablonski) diagram and treated as separate parallel and/or subsequent reactions or equilibria using conventional reaction kinetics. However, the short-time dynamics of prompt reactions and decay of Franck–Condon excited states is, up to a few picoseconds, determined by time-dependent quantum processes and an inertial solvent response [77,110,153,154]. The dynamics of the photoproduct formation calculated by the wavepacket propagation technique [77,110] are clearly different from the exponential kinetic profiles, well known from standard chemical kinetics. In this respect, the physical meaning of the activation energies and volumes determined experimentally for prompt photochemical reactions is somewhat obscure and needs further clarification.

From a more practical point of view, it is important to note that the prompt reactions release extremely rapidly highly reactive, coordinatively unsaturated, complexes, radicals or ligand fragments. They may be of importance in photocatalysis, photoimaging, photoinitiation of chain reactions, etc. Ultrafast isomerisation or electron transfer can be utilised in the development of molecular switches, or sensitisers for light energy conversion [149–152,155], respectively.

Chemical behaviour of MLCT states changes profoundly on going from the complexes of first row transition metals to those of heavier metals, especially of the third row. Their bonding interactions are rather long-ranging because of the more diffuse character of the 5d orbitals. Hence, the energy of the potentially dissociative states (LF, $\sigma\pi^*$) decreases only slowly with the metal–ligand distance. Moreover, the LF states lie rather high in energy because of a large ligand-field strength. The Franck–Condon excitation falls in the vicinity of a deep minimum on the MLCT energy surface. Any interaction between the MLCT and LF surfaces then occurs at rather high energies and at extensively distorted molecular geometries, if present at all. Such a situation is clearly very unfavourable for a prompt reaction. Instead, the

[4] LLCT stands for a ligand to ligand charge transfer excited state.

Franck–Condon excited state undergoes a vibrational and electronic relaxation to the lowest ^{3}MLCT state. Lifetimes of such relaxed states are often long enough (ns–μs) to allow excited molecules to equilibrate thermally, both internally and with their environment. Reactions of such long-lived, relaxed excited states may be treated as conventional thermal reactions using transition state theory and chemical kinetics. Relaxed ^{3}MLCT states have a much higher energy content and different electron distribution than the ground state. The charge separation between the metal and the acceptor ligand (Eq. (1)) is the most important difference. Indeed, the chemical reactivity of relaxed ^{3}MLCT states is essentially that of an oxidised metal atom or a reduced ligand.

The use of complexes with long-lived ^{3}MLCT states as photochemical oxidants and/or reductants is well known. It stems from the fact that the MLCT-active compounds often exhibit fast and reversible ground-state electron transfer reactions. In fact, a qualitative correlation between the stability of the reduced and/or oxidised forms of coordination and organometallic compounds and their ^{3}MLCT lifetime exists [84]. Excited state electron transfer reactions of long-lived ^{3}MLCT states are well understood [3,117–120,133,156]. They enable important applications of MLCT-active complexes as photosensitisers of light-energy conversion processes [3,119,136,157–162]. For example, the sensitiser used in the Grätzel photoelectrochemical cell is a MLCT-active supramolecular RuII polypyridyl complex, capable of both energy and electron transfer [163–165]. Moreover, it now appears [149–152] that the electron injection from an excited sensitiser to a semiconductor electrode can be an extremely fast, femtosecond, process. Hence, even complexes which have only short-lived MLCT states may be employed as sensitisers in solar cells, provided that their redox potentials are in a suitable range and that the coupling to the semiconductor surface is strong enough to allow for an ultrafast electron transfer. $[Fe(4,4'\text{-}(COOH)_2bpy)_2(CN)_2]$ is an excellent example of such a sensitiser [155]. Possible economic advantages over Ru or Os complexes are evident. Other applications of MLCT redox reactivity lie in studies of electron transfer reactions of metalloproteins [166–168], DNA photocleavage [169–173], or in a development of prospective molecular photonic materials for sensors [133,135,137,174–179].

Relaxed ^{3}MLCT states undergo associative reactions, provided that the metal centre is stericaly accessible. Quantum yields vary very much, from 10^{-6} to nearly 1, depending on the particular reaction. They may be moderately temperature dependent. An associative mechanism can be recognised unmistakably by a pressure dependence of the quantum yield which affords negative activation volumes [44,46,47]. Both ligand substitutions and oxidative additions are known. Photochemical oxidative additions are finding applications in photocatalysis. Their potential was already demonstrated by the photocatalysis of a carbonylation of hydrocarbons and by the water gas shift reaction using $Rh(PMe_3)_2(CO)(Cl)$ [71,72,127,128] and $[Cp^*Ir(phen)(Cl)]^+$ [129–131], respectively. Evidently, much more research on the photochemistry of MLCT-active coordinatively unsaturated complexes is needed.

The last mechanistic type discussed, a delayed ligand photodissociation, involves a reaction from a higher-lying reactive ^{3}LF excited state that is populated thermally from a relaxed ^{3}MLCT state, see Figs. 8 and 9. The ligand dissociation is delayed by the time needed for the relaxation of the initially excited Franck–Condon ^{1}MLCT state to the lowest ^{3}MLCT state and for the ^{3}MLCT → ^{3}LF conversion. The reaction is thus rather slow, taking place on a ns-μs timescale. The selectivity is determined entirely by the bonding properties of the ^{3}LF state. Quantum yields are low and strongly temperature-dependent with rather high activation energies, usually above 2500 cm^{-1}. Quantum yields depend on the excitation energy if there are close-lying LF and MLCT absorption bands in the spectrum. This type of MLCT reactivity is typical for coordination and organometallic compounds of metals from the second and third transition row. Complexes of the third row metals are often less reactive because of a larger ^{3}LF–^{3}MLCT energy gap.

Although the involvement of a higher reactive state in delayed photoreactivity may resemble prompt reactions, these two processes are physically completely different. The timescale of the delayed dissociation is slower by at least five orders of magnitude. A prompt reaction occurs as a propagation on that potential energy surface which was initially populated by the optical excitation and which is coupled with higher state(s) along the reaction coordinate. A delayed dissociation is, essentially, a thermal reaction of a relaxed ^{3}MLCT state. The initial MLCT excitation only pumps the light energy into the molecule and the ^{3}MLCT state acts as a sink in which the excitation energy is stored temporarily, until it is dissipated through a conversion to a higher, reactive, ^{3}LF state.

A delayed photosubstitution of MLCT-active complexes is often an unwanted reaction that could severely limit their use as photochemical sensitisers and catalysts. A lot of effort has been spent on the development of photochemically stable Ru^{II}–polypyridine complexes by tuning the energy separation between the ^{3}MLCT and ^{3}LF states [8,32,180] and/or by designing complexes with supramolecular cage-type acceptor ligands [133]. On the other hand, it is possible to employ a delayed MLCT photoreactivity in designing photochemically active organometallic compounds. One may envisage molecules which possess a reactive excited state that is difficult to populate optically because the corresponding electronic transition is too weak. An introduction of a MLCT chromophore into the molecule would provide an efficient indirect way to populate such a state. A release of highly reactive fragments, isomerisation, or intramolecular electron transfer may then follow within a ns–μs time interval after the excitation. The MLCT chromophore would play the role of an intramolecular light-absorption sensitiser.

Finally, MLCT states of many coordination and organometallic compounds are completely unreactive. Their only dynamic processes are a nonradiative and/or radiative decay to the ground state which, in supramolecular systems, may involve an intermolecular energy-transfer. Complexes with unreactive MLCT states are promising as materials for non-linear optics [181–184] and molecular electronics [133,185–189]. Photochemically stable polypyridyl complexes may be combined into polynuclear supramolecular assemblies or dendrimers that can act as molecular wires or broad-band light absorbers (antenna systems) through which the excitation energy may be channelled toward the reactive sites [133,156,159,186,190,191].

7. Conclusions

Metal-to-ligand charge-transfer, MLCT, excited states have a rich photochemistry. A MLCT excitation can activate molecules of organometallic or coordination compounds toward energy or electron transfer as well as toward reactions in which metal–ligand, metal–metal or intraligand bonds are broken, formed, or rearranged. In principle, MLCT excitation can have following photochemical consequences: (i) a prompt start of an ultrafast propagation toward the dissociated primary photoproduct, (ii) a creation of a long-lived, charge-separated, ^{3}MLCT state that shows typical reactivity of the oxidised metal atom or reduced ligand (electron transfer, associative substitution, oxidative addition), or (iii) a creation of a long-lived, unreactive, ^{3}MLCT state (energy sink) which temporarily stores the excitation energy until it is dissipated by a thermal population of another, more reactive, excited state. Alternatively, a MLCT state may be unreactive, just decaying to the ground state.

Depending on the structure of the photoreactive molecule and the medium, the rates of MLCT-induced reactions vary from femtoseconds to microseconds. The quantum yields change from as low as 10^{-6} to unity. An understanding of MLCT reactivity and dynamics requires to consider bonding properties of the initially excited (Franck–Condon) MLCT state, as well as relaxed ^{3}MLCT states and higher excited states of different orbital origins. The actual photochemistry is determined by potential energy curves of MLCT states and their interactions with other excited states along possible reaction coordinates, and by the rates of competitive deactivation processes.

Mechanistic studies of MLCT photochemistry afford deep understanding of the dynamics of excited states and chemical bonds, of structural and chemical effects of optically induced intramolecular charge separation and of secondary thermal reactions of primary photochemical products. Prompt reactions, which occur on a femtosecond timescale, are especially challenging from both experimental and theoretical points of view. Much research activity in the field of femtochemistry of MLCT-active complexes is expected in the near future. Further research on MLCT photochemistry will undoubtedly involve also a search for new photoactive complexes, aiming at applications in photocatalysis, light-energy conversion or molecular electronics. Several promising systems have already been reported.

Acknowledgements

Mr. I.R. Farrell (QMW) is gratefully thanked for his kind help with the manuscript preparation. This work was carried out within the European COST Project D4/0001/94 'Organometallic and Coordination Compounds Capable of Optical Charge-transfer Excitation: Design, Excited State Dynamics, Reactivity and Bistability'.

References

[1] G.L. Geoffroy, M.S. Wrighton, Organometallic Photochemistry, Academic Press, New York, 1979.
[2] A.B.P. Lever, Inorganic Electronic Spectroscopy, 2nd edn., Elsevier, Amsterdam, 1984.
[3] D.M. Roundhill, Photochemistry and Photophysics of Metal Complexes, Plenum Press, New York, 1994.
[4] G.J. Ferraudi, Elements of Inorganic Photochemistry, Wiley-Interscience, New York, 1988.
[5] O. Horvath, K.L. Stevenson, Charge Transfer Photochemistry of Coordination Compounds, VCH Publishers, New York, 1993.
[6] D.J. Stufkens, Coord. Chem. Rev. 104 (1990) 39.
[7] D.J. Stufkens, Comments Inorg. Chem. 13 (1992) 359.
[8] T.J. Meyer, Pure Appl. Chem. 58 (1986) 1193.
[9] A. Vogler, H. Kunkely, in: K. Kalyanasundaram, M. Grätzel (Eds.), Photosensitization and Photocatalysis Using Inorganic and Organometallic Compounds, Kluwer Academic Publishers, Dordrecht, 1993, p. 71.
[10] C. Creutz, M.D. Newton, N. Sutin, J. Photochem. Photobiol. A: Chem. 82 (1994) 47.
[11] Y.-g.K. Shin, B.S. Brunschwig, C. Creutz, N. Sutin, J. Phys. Chem. 100 (1996) 8157.
[12] P. Chen, K.M. Omberg, D.A. Kavaliunas, J.A. Treadway, R.A. Palmer, T.J. Meyer, Inorg. Chem. 36 (1997) 954.
[13] K.M. Omberg, J.R. Schoonover, J.A. Treadway, R.M. Leasure, R.B. Dyer, T.J. Meyer, J. Am. Chem. Soc. 119 (1997) 7013.
[14] J.V. Caspar, T.D. Westmoreland, G.H. Allen, P.G. Bradley, T.J. Meyer, W.H. Woodruff, J. Am. Chem. Soc. 106 (1984) 3492.
[15] G.A. Mines, J.A. Roberts, J.T. Hupp, Inorg. Chem. 31 (1992) 125.
[16] M.W. Kokkes, D.J. Stufkens, A. Oskam, J. Chem. Soc. Dalton Trans. (1983) 439.
[17] F. Hartl, A. Vlček Jr., Inorg. Chem. 31 (1992) 2869.
[18] G.F. Strouse, J.R. Schoonover, R. Duesing, S. Boyde, W.E. Jones, T.J. Meyer, Inorg. Chem. 34 (1995) 473.
[19] J.A. Treadway, B. Loeb, R. Lopez, P.A. Anderson, F.R. Keene, T.J. Meyer, Inorg. Chem. 35 (1996) 2242.
[20] N.H. Damrauer, T.R. Boussie, M. Devenney, J.K. McCusker, J. Am. Chem. Soc. 119 (1997) 8253.
[21] A. Vogler, H. Kunkely, Coord. Chem. Rev. 177 (1998) 81.
[22] P.C. Ford, R.E. Hintze, J.D. Petersen, in: A.W. Adamson, P.D. Fleischauer (Eds.), Concepts of Inorganic Photochemistry, Wiley-Interscience, New York, 1975, p. 203.
[23] P.C. Ford, in: M.S. Wrighton (Ed.), Inorganic and Organometallic Photochemistry, Advances in Chemistry Series 168, American Chemical Society, Washington, DC, 1978, p. 74.
[24] P.C. Ford, D. Wink, J. Di Benedetto, Prog. Inorg. Chem. 30 (1983) 213.
[25] M.S. Wrighton, D.L. Morse, J. Organomet. Chem. 97 (1975) 405.
[26] D.M. Manuta, A.J. Lees, Inorg. Chem. 25 (1986) 1354.
[27] H.K. van Dijk, D.J. Stufkens, A. Oskam, J. Am. Chem. Soc. 111 (1989) 541.
[28] G. Malouf, P.C. Ford, J. Am. Chem. Soc. 99 (1977) 7213.
[29] J. Van Houten, R.J. Watts, Inorg. Chem. 17 (1978) 3381.
[30] B. Durham, J.V. Caspar, J.K. Nagle, T.J. Meyer, J. Am. Chem. Soc. 104 (1982) 4803.
[31] J.V. Caspar, T.J. Meyer, J. Am. Chem. Soc. 105 (1983) 5583.
[32] D.P. Rillema, C.B. Blanton, R.J. Shaver, D.C. Jackman, M. Boldaji, S. Bundy, L.A. Worl, T.J. Meyer, Inorg. Chem. 31 (1992) 1600.
[33] M.S. Wrighton, H.B. Abrahamson, D.L. Morse, J. Am. Chem. Soc. 98 (1976) 4105.
[34] A.J. Lees, A.W. Adamson, J. Am. Chem. Soc. 104 (1982) 3804.
[35] S. Wieland, R. van Eldik, D.R. Crane, P.C. Ford, Inorg. Chem. 28 (1989) 3663.
[36] P. Glyn, F.P.A. Johnson, M.W. George, A.J. Lees, J.J. Turner, Inorg. Chem. 30 (1991) 3543.
[37] F.P.A. Johnson, M.W. George, J.J. Turner, Inorg. Chem. 32 (1993) 4226.
[38] V.W.-W. Yam, V.C.-Y. Lau, K.-K. Cheung, J. Chem. Soc., Chem. Commun. (1995) 259.

[39] J. Víchová, F. Hartl, A. Vlček Jr., J. Am. Chem. Soc. 114 (1992) 10903.
[40] A. Vlček Jr., J. Víchová, F. Hartl, Coord. Chem. Rev. 132 (1994) 167.
[41] I.G. Virrels, M.W. George, J.J. Turner, J. Peters, A. Vlček Jr., Organometallics 15 (1996) 4089.
[42] H.K. van Dijk, P.C. Servaas, D.J. Stufkens, A. Oskam, Inorg. Chim. Acta 104 (1985) 179.
[43] E. Lindsay, A. Vlček Jr., C.H. Langford, Inorg. Chem. 32 (1993) 2269.
[44] S. Wieland, K.B. Reddy, R. van Eldik, Organometallics 9 (1990) 1802.
[45] W.F. Fu, R. van Eldik, Inorg. Chim. Acta 251 (1996) 341.
[46] W.F. Fu, R. van Eldik, Organometallics 16 (1997) 572.
[47] W.-F. Fu, R. van Eldik, Inorg. Chem. 37 (1998) 1044.
[48] K.R. Mann, H.B. Gray, G.S. Hammond, J. Am. Chem. Soc. 99 (1977) 306.
[49] H.B. Gray, K.R. Mann, N.S. Lewis, J.A. Thich, R.M. Richman, in: M.S. Wrighton Jr. (Ed.), Inorganic and Organometallic Photochemistry, Advances in Chemistry Series 168, American Chemical Society, Washington, DC, 1978, p. 44.
[50] X. Xie, J.D. Simon, J. Phys. Chem. 93 (1989) 4401.
[51] E. Mašková, A. Vlček Jr., Inorg. Chim. Acta 242 (1996) 17.
[52] C.E. Johnson, W.C. Trogler, J. Am. Chem. Soc. 103 (1981) 6352.
[53] W.C. Trogler, in: A.B.P. Lever Jr. (Ed.), Excited States and Reactive Intermediates, ACS Symposium Series 307, American Chemical Society, Washington, DC, 1986, p. 177.
[54] G.J. Stor, S.L. Morrison, D.J. Stufkens, A. Oskam, Organometallics 13 (1994) 2641.
[55] C.J. Kleverlaan, F. Hartl, D.J. Stufkens, J. Photochem. Photobiol. A: Chem. 103 (1997) 231.
[56] B.D. Rossenaar, D.J. Stufkens, A. Oskam, J. Fraanje, K. Goubitz, Inorg. Chim. Acta 247 (1996) 215.
[57] K. Pierloot, E. Tsokos, L.G. Vanquickenborne, J. Phys. Chem. 100 (1996) 16545.
[58] C. Pollak, A. Rosa, E.J. Baerends, J. Am. Chem. Soc. 119 (1997) 7324.
[59] D.J. Stufkens, M.P. Aarnts, B.D. Rossenaar, A. Vlček Jr., Pure Appl. Chem. 69 (1997) 831.
[60] B.D. Rossenaar, C.J. Kleverlaan, D.J. Stufkens, A. Oskam, J. Chem. Soc., Chem. Commun. (1994) 63.
[61] B.D. Rossenaar, C.J. Kleverlaan, M.C.E. van de Ven, D.J. Stufkens, A. Vlček Jr., Chem. Eur. J. 2 (1996) 228.
[62] B.D. Rossenaar, M.W. George, F.P.A. Johnson, D.J. Stufkens, J.J. Turner, A. Vlček Jr., J. Am. Chem. Soc. 117 (1995) 11582.
[63] B.D. Rossenaar, E. Lindsay, D.J. Stufkens, A. Vlček Jr., Inorg. Chim. Acta 250 (1996) 5.
[64] C.J. Kleverlaan, D.M. Martino, H. van Willigen, D.J. Stufkens, A. Oskam, J. Phys. Chem. 100 (1996) 18607.
[65] J.W.M. van Outersterp, M.T.G. Oostenbrink, H.A. Nieuwenhuis, D.J. Stufkens, F. Hartl, Inorg. Chem. 34 (1995) 6312.
[66] J. Nijhoff, M.J. Bakker, F. Hartl, D.J. Stufkens, J. Organomet. Chem. (in press).
[67] J. Nijhoff, M.J. Bakker, F. Hartl, D.J. Stufkens, W.-F. Fu, R. van Eldik, Inorg. Chem. 37 (1998) 661.
[68] R.H. Hill, R.J. Puddephatt, J. Am. Chem. Soc. 107 (1985) 1218.
[69] D. Sandrini, M. Maestri, V. Balzani, L. Chassot, A. von Zelewsky, J. Am. Chem. Soc. 109 (1987) 7720.
[70] M. Maestri, V. Balzani, C. Deuschel-Cornioley, A. von Zelewsky, in: D. Volman, G. Hammond, D. Neckers (Eds.), Advances in Photochemistry, vol. 17, Wiley, New York, 1992, p. 1.
[71] G.P. Rosini, W.T. Boese, A.S. Goldman, J. Am. Chem. Soc. 116 (1994) 9498.
[72] S.E. Boyd, L.D. Field, M.G. Partridge, J. Am. Chem. Soc. 116 (1994) 9492.
[73] J.S. Bridgewater, B. Lee, S. Bernhard, J.R. Schoonover, P.C. Ford, Organometallics 16 (1997) 5592.
[74] E.J. Heller, Acc. Chem. Res. 14 (1981) 368.
[75] G.C. Schatz, M.A. Ratner, Quantum Mechanics in Chemistry, Prentice-Hall, Englewood Cliffs, NJ, 1993.
[76] R. Schinke, Photodissociation Dynamics, Cambridge University Press, New York, 1993.
[77] K. Finger, C. Daniel, P. Saalfrank, B. Schmidt, J. Phys. Chem. 100 (1996) 3368.

[78] K. Finger, C. Daniel, J. Am. Chem. Soc. 117 (1995) 12322.
[79] A. Rosa, G. Ricciardi, E.J. Baerends, D.J. Stufkens, Inorg. Chem. 34 (1995) 3425.
[80] A. Rosa, G. Ricciardi, E.J. Baerends, D.J. Stufkens, Inorg. Chem. 35 (1996) 2886.
[81] A. Rosa, G. Ricciardi, E.J. Baerends, D.J. Stufkens, J. Phys. Chem. 100 (1996) 15346.
[82] P.C. Servaas, D.J. Stufkens, A. Oskam, in: H. Yersin, A. Vogler (Eds.), Photochemistry and Photophysics of Coordination Compounds, Springer-Verlag, Berlin, 1987.
[83] I.R. Farrell, P. Matovšek, A. Vlček, Jr., Inorg. Chem. (in press).
[84] A. Vlček Jr., Chemtracts-Inorg. Chem. 5 (1993) 1.
[85] D. Miholová, A.A. Vlček, J. Organomet. Chem. 279 (1985) 317.
[86] J. Hanzlik, L. Pospíšil, A.A. Vlček, M. Krejčík, J. Electroanal. Chem. 331 (1992) 831.
[87] R.W. Balk, T. Snoeck, D.J. Stufkens, A. Oskam, Inorg. Chem. 19 (1980) 3015.
[88] D. Guillaumont, C. Daniel, Coord. Chem. Rev. 177 (1998) 181.
[89] A. Messiah, Quantum Mechanics, Ch. III.6, vol. 1, North-Holland, Amsterdam, 1963.
[90] D.J. Stufkens, A. Vlček Jr., Coord. Chem. Rev. 177 (1998) 127.
[91] C.J. Kleverlaan, D.J. Stufkens, J. Photochem. Photobiol. A: 116 (1998) 109.
[92] S. Campagna, G. Denti, G. De Rosa, L. Sabatino, M. Ciano, V. Balzani, Inorg. Chem. 28 (1989) 2565.
[93] H. Kunkely, A. Vogler, Inorg. Chim. Acta 250 (1996) 375.
[94] H. Kunkely, A. Vogler, Inorg. Chim. Acta 256 (1997) 169.
[95] H. Kunkely, A. Vogler, Chem. Commun. (1996) 2519.
[96] T. Lian, S.E. Bromberg, M.C. Asplund, H. Yang, C.B. Harris, J. Phys. Chem. 100 (1996) 11994.
[97] A.G. Joly, K.A. Nelson, Chem. Phys. 152 (1991) 69.
[98] N.A. Beach, H.B. Gray, J. Am. Chem. Soc. 90 (1968) 5713.
[99] K.R. Mann, M. Cimolino, G.L. Geoffroy, G.S. Hammond, A.A. Orio, G. Albertin, H.B. Gray, Inorg. Chim. Acta 16 (1976) 97.
[100] F.P.A. Johnson, M.W. George, S.L. Morrison, J.J. Turner, J. Chem. Soc., Chem. Commun. (1995) 391.
[101] D.L. Morse, M.S. Wrighton, J. Am. Chem. Soc. 98 (1976) 3931.
[102] R.R. Andrea, W.G.J. de Lange, D.J. Stufkens, A. Oskam, Inorg. Chem. 28 (1989) 318.
[103] M.W. Kokkes, D.J. Stufkens, A. Oskam, Inorg. Chem. 24 (1985) 2934.
[104] M.P. Aarnts, D.J. Stufkens, A. Vlček Jr., Inorg. Chim. Acta 266 (1997) 37.
[105] H.A. Nieuwenhuis, A. van Loon, M.A. Moraal, D.J. Stufkens, A. Oskam, K. Goubitz, J. Organomet. Chem. 492 (1995) 165.
[106] H.A. Nieuwenhuis, M.C.E. van de Ven, D.J. Stufkens, A. Oskam, K. Goubitz, Organometallics 14 (1995) 780.
[107] I.R. Farrell, A. Vlček, Jr. (in press).
[108] M.P. Aarnts, D.J. Stufkens, M.P. Wilms, E.J. Baerends, A. Vlček Jr., I.P. Clark, J.J. Turner, Chem. Eur. J. 2 (1996) 1556.
[109] M.W. Kokkes, T.L. Snoeck, D.J. Stufkens, A. Oskam, M. Cristophersen, C.H. Stam, J. Mol. Struct. 131 (1985) 11.
[110] D. Guillaumont, K. Finger, M.R. Hachey, C. Daniel, Coord. Chem. Rev. 171 (1998) 439.
[111] M.P. Aarnts, M.P. Wilms, D.J. Stufkens, E.J. Baerends, A. Vlček Jr., Organometallics 16 (1997) 2055.
[112] M.P. Aarnts, M.P. Wilms, K. Peelen, J. Fraanje, K. Goubitz, F. Hartl, D.J. Stufkens, E.J. Baerends, A. Vlček Jr., Inorg. Chem. 35 (1996) 5468.
[113] C.J. Kleverlaan, D.J. Stufkens, I.P. Clark, M.W. George, J.J. Turner, D.M. Martino, H. van Willigen, A. Vlček Jr., J. Am. Chem. Soc. 120 (1998) 10871.
[114] S. Hasenzahl, H.-D. Hausen, W. Kaim, Chem. Eur. J. 1 (1995) 95.
[115] W. Kaim, A. Klein, S. Hasenzahl, H. Stoll, S. Záliš, J. Fiedler, Organometallics 17 (1998) 237.
[116] E. Wissing, E. Rijnberg, P.A. van der Schaaf, K. van Gorp, J. Boersma, G. van Koten, Organometallics 13 (1994) 2609.
[117] V. Balzani, F. Bolletta, M.T. Gandolfi, M. Maestri, Top. Curr. Chem. 75 (1978) 1.
[118] V. Balzani, F. Bolletta, F. Scandola, R. Ballardini, Pure Appl. Chem. 51 (1979) 299.
[119] V. Balzani, F. Barigelletti, L. De Cola, Top. Curr. Chem. 158 (1990) 31.

[120] V. Balzani, M. Maestri, in: K. Kalyanasundaram, M. Grätzel (Eds.), Photosensitization and Photocatalysis Using Inorganic and Organometallic Compounds, Kluwer Academic Publishers, Dordrecht, 1993, p. 15.
[121] K.-T. Wan, C.M. Che, J. Chem. Soc., Chem. Commun. (1990) 140.
[122] M. Ruthkosky, F.N. Castellano, G.J. Meyer, Inorg. Chem. 35 (1996) 6406.
[123] P. Holzmeier, H. Gorner, F. Knoch, H. Kisch, Chem. Ber. 122 (1989) 1457.
[124] W.F. Fu, H. Kisch, R. van Eldik, Organometallics 16 (1997) 3439.
[125] P.C. Servaas, W.G.J. De Lange, D.J. Stufkens, A. Oskam, Inorg. Chim. Acta 173 (1990) 175.
[126] A. von Zelewsky, A.P. Suckling, H. Stoeckli-Evans, Inorg. Chem. 32 (1993) 4585.
[127] G.P. Rosini, K. Zhu, A.S. Goldman, J. Organomet. Chem. 504 (1995) 115.
[128] M.G. Partridge, L.D. Field, B.A. Messerle, Organometallics 15 (1996) 872.
[129] R. Ziessel, J. Chem. Soc., Chem. Commun. (1988) 16.
[130] R. Ziessel, Angew. Chem. Int. Ed. Engl. 30 (1991) 844.
[131] R. Ziessel, J. Am. Chem. Soc. 115 (1993) 118.
[132] D. Sandrini, M. Maestri, R. Ziessel, Inorg. Chim. Acta 163 (1989) 177.
[133] V. Balzani, F. Scandola, Supramolecular Photochemistry, Ellis Horwood, Chichester, 1991.
[134] F. Casalboni, Q.G. Mulazzani, C.D. Clark, M.Z. Hoffman, P.L. Orizondo, M.W. Perkovic, D.P. Rillema, Inorg. Chem. 36 (1997) 2252.
[135] R. Grigg, J.M. Holmes, S.K. Jones, W.D.J.A. Norbert, J. Chem. Soc., Chem. Commun. (1994) 185.
[136] M.K. Nazeeruddin, E. Muller, R. Humphry-Baker, N. Vlachopoulos, M. Grätzel, J. Chem. Soc. Dalton Trans. (1997) 4571.
[137] J.M. Price, W. Xu, J.N. Demas, B.A. DeGraff, Anal. Chem. 70 (1998) 265.
[138] A. Vogler, J. Kisslinger, W.R. Roper, Z. Naturforsch. 38b (1983) 1506.
[139] R.M. Kolodziej, A.J. Lees, Organometallics 5 (1986) 450.
[140] K.A. Rawlins, A.J. Lees, A.W. Adamson, Inorg. Chem. 29 (1990) 3866.
[141] A.J. Lees, A.W. Adamson, J. Am. Chem. Soc. 102 (1980) 6874.
[142] E. Lindsay, A. Vlček Jr., C.H. Langford, Inorg. Chem. 32 (1993) 3822.
[143] J.E. Figard, J.D. Petersen, Inorg. Chem. 17 (1978) 1059.
[144] S. Chun, E.E. Getty, A.J. Lees, Inorg. Chem. 23 (1984) 2155.
[145] J. Van Houten, R.J. Watts, J. Am. Chem. Soc. 98 (1976) 4853.
[146] W.E. Jones Jr., R.A. Smith, M.T. Abramo, M.D. Williams, J. Van Houten, Inorg. Chem. 28 (1989) 2281.
[147] H.B. Ross, M. Boldaji, D.P. Rillema, C.B. Blanton, R.P. White, Inorg. Chem. 28 (1989) 1013.
[148] F.N. Castellano, H. Malak, I. Gryczynski, J.R. Lakowicz, Inorg. Chem. 36 (1997) 5548.
[149] J.Z. Zhang, Acc. Chem. Res. 30 (1997) 423.
[150] T. Hannappel, B. Burfeindt, W. Storck, F. Willig, J. Phys. Chem. B 101 (1997) 6799.
[151] N.J. Cherepy, G.P. Smestad, M. Grätzel, J.Z. Zhang, J. Phys. Chem. B 101 (1997) 9342.
[152] Y. Tachibana, J.E. Moser, M. Grätzel, D.R. Klug, J.R. Durrant, J. Phys. Chem. 100 (1996) 20056.
[153] N.H. Damrauer, G. Cerullo, A. Yeh, T.R. Boussie, C.V. Shank, J.K. McCusker, Science 275 (1997) 54.
[154] J.P. Cushing, C. Butoi, D.F. Kelley, J. Phys. Chem. A. 101 (1997) 7222.
[155] S. Ferrere, B.A. Gregg, J. Am. Chem. Soc. 120 (1998) 843.
[156] F. Scandola, C.A. Bignozzi, M.T. Indelli, in: K. Kalyanasundaram, M. Grätzel (Eds.), Photosensitization and Photocatalysis Using Inorganic and Organometallic Compounds, Kluwer Academic Publishers, Dordrecht, 1993, p. 161.
[157] E. Amouyal, Sol. Energy Mater. Sol. Cells 38 (1995) 249.
[158] A.J. Bard, M.A. Fox, Acc. Chem. Res. 28 (1995) 141.
[159] C.A. Bignozzi, J.R. Schoonover, F. Scandola, Progr. Inorg. Chem. 44 (1997) 1.
[160] K. Kalyanasundaram, in: K. Kalyanasundaram, M. Grätzel (Eds.), Photosensitization and Photocatalysis Using Inorganic and Organometallic Compounds, Kluwer Academic Publishers, Dordrecht, 1993, p. 113.
[161] O. Kohle, S. Ruile, M. Grätzel, Inorg. Chem. 35 (1996) 4779.

[162] S.M. Zakeeruddin, M.K. Nazeeruddin, P. Pechy, F.P. Rotzinger, R. Humphry-Baker, K. Kalyanasundaram, M. Grätzel, V. Shklover, T. Haibach, Inorg. Chem. 36 (1997) 5937.
[163] B. O'Regan, M. Grätzel, Nature 353 (1991) 737.
[164] M. Grätzel, K. Kalyanasundaram, in: K. Kalyanasundaram, M. Grätzel (Eds.), Photosensitization and Photocatalysis Using Inorganic and Organometallic Compounds, Kluwer Academic Publishers, Dordrecht, 1993, p. 247.
[165] M. Grätzel, Coord. Chem. Rev. 111 (1991) 167.
[166] H.B. Gray, W.R. Ellis Jr., in: I. Bertini, H.B. Gray, S.J. Lippard, J.S. Valentine (Eds.), Bioinorganic Chemistry, University Science Books, Mill Valley, CA, 1994.
[167] J.R. Winkler, H.B. Gray, Chem. Rev. 92 (1992) 369.
[168] H.B. Gray, J.R. Winkler, Annu. Rev. Biochem. 65 (1996) 537.
[169] J.K. Barton, in: I. Bertini, H.B. Gray, S.J. Lippard, J.S. Valentine (Eds.), Bioinorganic Chemistry, University Science Books, Mill Valley, CA, 1994, p. 455.
[170] H.D. Stoeffler, N.B. Thornton, S.L. Temkin, K.S. Schanze, J. Am. Chem. Soc. 117 (1995) 7119.
[171] V.W.-W. Yam, K.K.-W. Lo, K.-K. Cheung, R.Y.-C. Kong, J. Chem. Soc., Chem. Commun. (1995) 1191.
[172] V.W.-W. Yam, K.K.-W. Lo, K.-K. Cheung, R.Y.-C. Kong, J. Chem. Soc., Dalton Trans. (1997) 2067.
[173] E.J.C. Olson, D. Hu, A. Hormann, A.M. Jonkman, M.R. Arkin, E.D.A. Stemp, J.K. Barton, P.F. Barbara, J. Am. Chem. Soc. 119 (1997) 11458.
[174] V.W.-W. Yam, K.M.-C. Wong, V.W.-M. Lee, K.K.-W. Lo, K.-K. Cheung, Organometallics 14 (1995) 4034.
[175] D.I. Yoon, C.A. Berg-Brennan, H. Lu, J.T. Hupp, Inorg. Chem. 31 (1992) 3192.
[176] C.A. Berg-Brennan, D.I. Yoon, R.V. Slone, A.P. Kazala, J.T. Hupp, Inorg. Chem. 35 (1996) 2032.
[177] P.D. Beer, Z. Chen, A.J. Goulden, A. Grieve, D. Hesek, F. Szemes, T. Wear, J. Chem. Soc., Chem. Commun. (1994) 1269.
[178] P.D. Beer, S.W. Dent, T.J. Wear, J. Chem. Soc., Dalton Trans. (1996) 2341.
[179] V.W.-W. Yam, V.W.-M. Lee, F. Ke, K.-W.M. Siu, Inorg. Chem. 36 (1997) 2124.
[180] C.D. Clark, M.Z. Hoffman, D.P. Rillema, Q.G. Mulazzani, J. Photochem. Photobiol. A: Chem. 110 (1997) 285.
[181] J.C. Calabrese, W. Tam, Chem. Phys. Lett. 133 (1987) 244.
[182] C. Dhenaut, I. Ledoux, I.D.W. Samuel, J. Zyss, M. Bourgault, H. Le Bozec, Nature 374 (1995) 339.
[183] M. Bourgault, C. Mountassir, H. Le Bozec, I. Ledoux, G. Pucetti, J. Zyss, J. Chem. Soc., Chem. Commun. (1993) 1623.
[184] B.J. Coe, M.C. Chamberlain, J.P. Essex-Lopresti, S. Gaines, J.C. Jeffery, S. Houbrechts, A. Persooms, Inorg. Chem. 36 (1997) 3284.
[185] V. Goulle, A. Harriman, J.-M. Lehn, J. Chem. Soc., Chem. Commun. (1993) 1034.
[186] A. Harriman, R. Ziessel, Chem. Commun. (1996) 1707.
[187] V.W.-W. Yam, V.C.-Y. Lau, K.-K. Cheung, Organometallics 14 (1995) 2749.
[188] V.W.-W. Yam, V.C.-Y. Lau, K.-K. Cheung, Organometallics 15 (1996) 1740.
[189] A. Beyeler, P. Belser, L. De Cola, Angew. Chem. Int. Ed. Engl. 36 (1997) 2779.
[190] S. Campagna, G. Denti, S. Serroni, A. Juris, M. Venturi, V. Ricevuto, V. Balzani, Chem. Eur. J. 1 (1995) 211.
[191] E.C. Constable, Chem. Commun. (1997) 1073.